Helsinki University of Technology
Department of Chemical Technology
Laboratory of Physical Chemistry and Electrochemistry
Espoo 2003

ELECTROCHEMICAL AND PHYSICOCHEMICAL CHARACTERIZATION OF RADIATION-GRAFTED MEMBRANES FOR FUEL CELLS

Tanja Kallio

TEKNILLINEN KORKEAKOULU
TEKNISKA HÖGSKOLAN
HELSINKI UNIVERSITY OF TECHNOLOGY
TECHNISCHE UNIVERSITÄT HELSINKI
UNIVERSITE DE TECHNOLOGIE D'HELSINKI

Helsinki University of Technology
Department of Chemical Technology
Laboratory of Physical Chemistry and Electrochemistry
Espoo 2003

ELECTROCHEMICAL AND PHYSICOCHEMICAL CHARACTERIZATION OF RADIATION-GRAFTED MEMBRANES FOR FUEL CELLS

Tanja Kallio

Dissertation for the degree of Doctor of Science in Technology to be presented with due permission of the Department of Chemical Technology, for public examination and debate in Komppa Auditorium at Helsinki University of Technology (Espoo, Finland) on the 18th of October, 2003, at 12 noon.

ISBN 951-22-6752-7 (printed)
ISBN 951-22-6753-5 (URL: http://lib.hut.fi/Diss/)

Edita Prima Oy
Helsinki 2003

Abstract

This thesis considers alternative proton conducting membrane materials for polymer electrolyte fuel cells (PEFC). The membrane is a key component of the PEFC accounting for the separation of the reactants and allowing the transport of hydrogen ions produced by the anode reaction to the cathode for the cathode reaction while enforcing the electrons to move through the external circuit so that the electrical energy can be utilized.

Here the applicability of radiation-grafted membranes in the PEFC with hydrogen or methanol as a fuel has been considered. In particular, the influence of the matrix material of a radiation-grafted membrane on its the behaviour is clarified. The experimental membranes studied were prepared from fluoropolymer films by irradiating with an electron beam, subsequently grafting with styrene and finally sulfonating. Poly(vinylidene fluoride) PVDF, poly(vinylidene fluoride-*co*-hexafluoropropylene), PVDF-co-HFP, poly(ethylene-*alt*-tetrafluoroethylene), ETFE and poly(tetrafluoroethylene-*co*-hexafluopropylene), FEP, were chosen as matrix fluoropolymers. In addition the effect of thickness of the matrix was examined with three PVDF films.

Scanning electrochemical microscopy was used as a new tool to investigate proton transport and distribution in the ionically conducting membranes. Such essential membrane properties as conductivity, oxygen permeability, water drag coefficients, methanol permeability, and the actual performance under the fuel cell conditions were found to depend on the crystallinity, or, more precisely, on the water uptake of the membrane, which was higher in membranes with lower crystallinity.

The degradation of the side chains ensuring the protonic conductivity was one of the problems restricting the lifetime of the radiation-grafted membranes in the fuel cell with hydrogen as a fuel. However, also the ability of the matrix material itself to withstand this aggressive environment by sustaining the pristine structural arrangement appeared to affect the membrane durability. In general, it appeared that crystallites and a greater matrix thickness brought more strength, provided the matrix did not suffer from phase changes. Using a bis(vinyl phenyl)ethane crosslinker for the PVDF based membranes was detected to protect the side of the membrane facing the anode from chemical degradation. However, no significant improvement in the membrane lifetime was attained due to the degradation of the cathode side of the membrane, with a resulting loss of protonic conductivity.

When using methanol as a fuel it was observed that similar performances to commercial materials could be achieved with the radiation-grafted membranes despite of their lower conductivities. This was attributed to the lower methanol permeability of the radiation-grafted membranes due to slower methanol diffusion through the membranes as a consequence of differences in the structures of the membranes.

Preface

This work was carried out at the Laboratory of Physical Chemistry and Electrochemistry, Helsinki University of Technology, Finland from June 1998 to May 2003.

I wish to express my gratitude to the head of the laboratory, professor Kyösti Kontturi, for interest in my work. I would also like to thank for emeritus professor Göran Sundholm for guidance and encouragement throughout my research as well as supervision of my studies.

The invaluable contributions of my co-authors have been most welcome. Especially Dr. Nadia Walsby, Peter Holmlund, M.Sc., and Dr. Tero Lehtinen are thanked for numerous fruitful discussions and collaboration. I am grateful to Dr. Hanna Erickson at Chalmers University of Technology for Raman characterization and to Dr. Ritva Serimaa and Dr. Kaija Jokela at University of Helsinki for the X-ray measurements and discussions related to these subjects. Dr. Sami Hietala and Dr. Sirkka Liisa Maunu are acknowledged for the NMR measurements. I would also like to thank Dr. Christofer Slevin for his guidance and help with the SECM measurements. Dr. Franciska Sundholm is also acknowledged for interst in this work.

The different facets of membrane characterization have allowed me to meet many people at Helsinki University of Technology, Åbo Academy University, University of Helsinki, Royal Institute of Technology, and National Research Centre, in addition to those already named. I wish to thank these research colleagues for discussions and collaborative operation.

Research colleagues and permanent staff in the laboratory of Physical Chemistry and Electrochemistry are thanked for helpful and encouraging working atmosphere.

The Academy of Finland (EMMA Electronic Materials and Microsystems and MATRA Materials and Structure Research programmes), the Magnus Ehrnrooth foundation as well as the National Technology Agency (Finland) are acknowledged for financial support.

Espoo, 12th May 2003

Tanja Kallio

Contents

List of Publications

This thesis includes the following papers, which are referred in the text by their Roman numerals:

I N. Walsby, F. Sundholm, T. Kallio and G. Sundholm, Radiation-grafted ion-exchange membranes. Influence of the Initial Matrix on the Synthesis, Structure and Non-transport Properties., *J. Polym. Sci. Part A: Polym. Chem.*, **39** (2001) 3008-3017.

II H. Ericson, T. Kallio, T. Lehtinen, N. Walsby, G. Sundholm, F. Sundholm and P. Jacobsson, Confocal Raman Spectroscopic Investigations of Fuel Cell Tested Sulfonated Styrene Grafted PVDF Membranes, *J. Electrochem. Soc*., **149** (2002) A206-A211.

III N. Walsby, S. Hietala. S.L. Maunu, F. Sundholm, T. Kallio and G. Sundholm, Water in Different Polystyrene Sulfonic Acid Grafted Fluoropolymers, *J. Appl. Polym. Sci*., **86** (2002) 33-42.

IV T. Kallio, M. Lundström, G. Sundholm, N. Walsby and F. Sundholm, Electrochemical Characterization of Radiation-grafted Ion-exchange Membranes Based on Different Matrix Polymers, *J. Appl. Electrochem*., **32** (2002) 11-18.

V T. Kallio, K. Jokela, R. Serimaa, H. Ericson, G. Sundholm, P. Jacobsson and F. Sundholm, The Effect of Fuel Cell Test on the Structure of Radiation-grafted Ion-exchange Membranes Based on Different Fluoropolymers., *J. Appl. Electrochem.*, **33** (2003) 505-514.

VI T. Kallio, C. Slevin, G. Sundholm, P. Holmlund and Kyösti Kontturi, Proton Transport in Radiation-grafted Membranes for Fuel Cells as Detected by SECM, *Electrochem. Comm.*, **5** (2003) 561-565.

This thesis also includes previously unpublished work regarding methanol permeability through the experimental membranes and their applicability in a direct methanol fuel cell.

Statement of the Author's Role in the listed publications

In publications I, II and III Tanja Kallio has done the AFM as well as the physicochemical and the electrochemical measurements. She has taken active part in interpreting the results and writing these papers. The experimental work presented in publication IV, V and VI has been done by Kallio excluding the Raman and the X-ray measurement, which have been performed at Chalmers University of Technology and at University of Helsinki. She has been the principal author of these publications. In addition to these papers, the thesis contains unpublished results on membranes in a small-scale fuel cell and methanol permeability measurements through the membranes performed by the author.

Espoo, 20th May 2003

Kyösti Kontturi
professor

1. Introduction

A fuel cell is an electrochemical device where the chemical energy of compounds is directly converted into electrical energy via electrochemical reactions. Unlike a conventional battery, a fuel cell is not an energy-storing apparatus but reactants are fed into the cell separately and continuously during the operation. A hydrogen rich compound or pure hydrogen is used as a fuel, while oxygen from the air commonly serves as oxidant. The benefits obtained using a fuel cell for energy production are high efficiency and low emissions: the electrical energy is produced directly, *i.e.* avoiding the low efficiency conversion of thermal to mechanical energy occurring in thermomechanical engines, and the only product is water if pure hydrogen is used.

In a polymer electrolyte fuel cell (PEFC) an ion exchange polymer membrane functions as an electrolyte offering a path for the ionic species emerged from the electrochemical reactions to migrate from the fuel to the oxidant compartments while forcing the produced electrons to move trough the external circuit so that the electrical energy can be utilized. The membrane also separates the reactants from each other. The currently commercially available membranes perform well but are expensive and contribute significantly to the overall cost of the system. The high price of the fuel cell components remains one of the main obstacles to commercialization of fuel cells.

Although fuel cells are only nowadays gaining commercial interest, the principle of operation was discovered already in 1838-1845 as a result of a dialogue between Christian Schoenbein and William Grove [1]. The former gentleman was the father of the fuel cell effect while to W. Grove is attributed the engineering work. He eventually constructed an operating cell consisting of continuous feed of hydrogen and oxygen reactants to platinum electrodes and a sulfuric acid solution as an electrolyte. Since those days the development of fuel cell devices continued with long intervals until Francis Bacon embarked on engineering a cell with an alkaline electrolyte and inexpensive nickel based electrodes in 1932 [2]. After this invention research on fuel cells acquired new impetus leading to the invention of new cell assemblages, including PEFCs as a result of development work at General Electric (USA) during the 1950s [3]. The PEFCs proved their power as an energy source in the Gemini spacecraft during the early 1960s but their usage was restricted only to special applications, such as the aforementioned spacecrafts and submarines [4].

During the last decades increasing environmental concerns and progress in the fuel cell technology, for example the introduction of the durable Nafion® membrane by DuPoint (USA) and the reduction of the amount of precious platinum catalyst in the electrodes, have awakened general interest in the PEFCs. Hence models applicable mainly for

automotive and stationary applications started to be developed during the 1980s [5] resulting in trial runs of bus [6,7] and car prototypes [7-9] and, at present the first cars are on the market [10]. In addition, in recent years small-scale PEFCs to replace batteries in portable applications, such as video cameras and laptop computers, have been brought into focus [7,10-12].

At the turn of the 20^{th} and the 21^{st} century the world total annual energy production was over 10^{14} kWh, of which 85 % was produced from fossil fuels releasing large amounts of carbon dioxide and other contaminants into the atmosphere [13]. Even though in the first stage fuel cells could not free man from fossil fuels – hydrogen will have to come from somewhere - they could improve the air quality in large cities, where pollution from the exhaust gases is intolerably high. Sooner or later the fossil fuel reserves will end but hydrogen, the fuel for fuel cells, could be obtained from other sources, for example by water electrolysis, which would reduce pollution problems significantly.

2. Background

2.1 Fuel cell types classified on the basis of the electrolyte

The electrolyte is one of the key components of the fuel cell and affects the choice of such parameters as the electrocatalysts and the operation temperature region. Fuel cells are usually classified into five categories on the basis of the electrolyte [14]:

In a polymer electrolyte fuel cell (PEFC) a proton conducting polymer membrane serves as an electrolyte. Since the only liquid in this type of fuel cell is water, corrosion is low. However, the water management is difficult since the commonly used membranes require water for the proton conductivity, but extra water may block the reactant gas access to the electrodes. Also expensive noble metal catalysts, which are sensitive to some compounds possibly present in the reactants, are required due to the low operation temperature combined with the acidic environment.

In addition to hydrogen, liquid methanol has also been considered as a fuel for PEFC. If methanol is directly fed to the fuel cell where it electrooxidizes, the device is known as a direct methanol fuel cell (DMFC). The main advantage achieved with methanol, compared to hydrogen, is the easier storage and delivery of the fuel. However, the methanol reaction is more sluggish and permeability of methanol through the membrane, from the anode to the cathode, decreases the efficiency of the cell due to thus formed mixed potentials at the cathode. In addition, some of the fuel is wasted.

In an alkaline fuel cell the typical ionic conductor is a concentrated KOH solution and the operation temperature is $<120^{o}C$ or $\sim250^{o}C$ depending on the concentration of the electrolyte. This cell offers the possibility to use a wide range of non precious electrocatalysts. A drawback is that the alkaline electrolyte reacts with the CO_2 remains in the reactants, changing the structure of the electrolyte, which results in a decrease in the OH^- ion conductivity by formation of solid carbonates in the cell. The use of a liquid electrolyte in general induces problems with corrosion and with maintaining the electrolyte in its place.

A phosphoric acid fuel cell utilizes acid retained in a silicon carbide matrix as an electrolyte and attains sufficient H^+ conductivity at a temperature of $150\text{-}200^{o}C$. Thanks to higher operation temperature this cell tolerates catalyst poisons somewhat better than the PEFC. However, the current density is lower than in the PEFC and the combination of an acidic environment and a relatively low operating temperature at present requires the use of expensive platinum catalysts. The liquid electrolyte brings the problems of corrosion and leaking as in the case of the alkaline fuel cell.

Alkaline carbonates retained in a ceramic matrix of $LiAlO_2$ usually function as an electrolyte in a molten carbonate fuel cell, which operates at a high temperature of 600 to 700^{o}C. At these temperatures alkaline carbonates form conducting molten salts with carbonate ions as moving species and no noble metal catalyst is needed. In addition the high operation temperature allows the reforming of fuels in the cell and high quality heat is obtained as a side product. However, the molten alkaline electrolyte environment is corrosive and problems with leaking of the electrolyte exist.

The operating temperature range of the solid oxide fuel cell is from 600 up to 1000^{o}C since oxygen ion conduction of the nonporous metal oxide electrolyte, typically Y_2O_3 stabilized ZrO_2, is sufficient only at these high temperatures. This cell type has the same benefits as the molten carbonate fuel cell operating at high temperatures but, in addition, the ceramic oxide is not corrosive. However, the construction of a working fuel cell stack has proved to be very difficult because of problems with the thermal compatibility of the materials.

2.2 Principle of operation of a polymer electrolyte fuel cell

In a typical PEFC a membrane with sulfonic acid cation exchange groups are utilized and, therefore, the reactions take place under strongly acidic conditions as is sketched in Figure 1. The fuel, in general hydrogen or a hydrogen rich gas, is fed to the anode, where it is oxidized on the platinum electrocatalyst according to the following reaction:

$$H_2 \rightarrow 2\ H^+ + 2\ e^- \qquad E^\circ = 0.000\ V \qquad \text{(i)}$$

Another possibility is to use methanol or some other hydrogen containing liquid as a fuel. Operation of this type of PEFC is described in Chapter 5.

The cathode, likewise electrocatalysed with platinum, is fed with an oxidant, normally oxygen from air. At this electrode electrons and protons are combined with oxygen producing water:

$$4\ H^+ + 4\ e^- + O_2 \rightarrow 2\ H_2O \qquad E^\circ = 1.229\ V \qquad \text{(ii)}$$

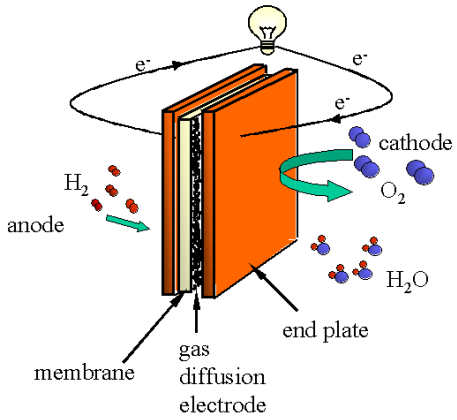

Figure 1. Scheme of a PEFC. Hydrogen, the fuel, is oxidized at the anode according to reaction (i), and the protons formed are transported to the cathode through the polymer electrolyte while the electrons are conducted via the external circuit to the cathode where both react with oxygen according to reaction (ii).

When the cell is connected to an external load, electrons produced at the anode are transported along the external circuit providing electric current. Meanwhile the protons are 1transported to the cathode through the polymer electrolyte in the electric field brought about by the potential difference between the electrodes. Electric current, heat, and water are obtained as products according to the overall reaction:

$$H_2 + 1/2\ O_2 \rightarrow H_2O \qquad \text{(iii)}$$

Under standard conditions (298 K, 1 atm) the reversible potential of this reaction is 1.23 V with liquid water as a product. The open circuit potential (OCP) of a fuel cell should be close to that but in fact lower values are obtained because of kinetic limitations of the electrode reactions, especially that of the oxygen [15]. Also composition and purity of the reactants, water equilibrium in the membrane electrode assembly, as well as permeation of the reactants through the membrane affect the OCP.

In practice the relation between the obtained potential and current is determined, in addition to the above mentioned activation overpotentials, $\eta_{i,act}$, by the ohmic resistance of the components or *IR* losses, as well as mass transport limitations, $\eta_{i,mt}$, due to, among other things, hindered transport of the reactants to the electrodes as a consequence of the accumulation of the produced water. An idea of the voltage current dependence can be obtained from equation (1) describing the main loss terms:

$$E = E^{\circ} - IR - \left|\eta_{A,act} + \eta_{A,mt}\right| - \left|\eta_{C,act} + \eta_{C,mt}\right| \quad (1)$$

where subscript A refers to the anode and C to the cathode. The overpotentials met on the cathode are substantially higher than those in the anode.

2.3 Solid polymer electrolyte membranes

In order to be a feasible candidate for the fuel cell the membrane should conform to several requirements set by the operating principle of a fuel cell combined with the aggressive operating environment and the requirements of commercialization. These are generally agreed to include:

- chemical and electrochemical stability under the fuel cell operation conditions and during the construction of the membrane electrode assembly
- mechanical and dimensional stability
- high proton conductivity combined with low area resistance, a value of 0.5 Ω cm^2 has been proposed for all of the fuel cell components together [40] while 0.1 Ω cm^2 has been suggested for the membrane itself at the operating temperature of the cell [16]
- appropriate water transport properties to prevent localized drying (in currently used membranes where the proton conductivity depends on the membrane water content)
- impermeable to reactants
- compatibility with the other fuel cell components, especially appropriate surface properties for combination with the electrodes
- low cost

The idea of using cation exchange polymer membranes as an electrolyte in fuel cells dates back to the late 1950s [3,17]. At that time several membrane candidates existed including sulfonated phenolformaldehyde compounds and divinyl benzene crosslinked polystyrene sulfonic acid embedded in a polymer film. However, these early competitors suffered from poor stability, a problem which was not solved until the introduction of Nafion® membranes in the late 1960s. The perfluorinated backbone with flexible ether linkages containing perfluorinated side chains terminating in a strongly acidic sulfonated group proved to be a durable concept.

Nevertheless, the high price due to the complicated synthesis process of these membranes has pushed forward research and development of alternative materials. The choice of the electrolyte membrane may affect the total cost of a fuel cell remarkably since estimations about the share of the polymer electrolyte in the total cost of a future fuel cell stack vary between 2 % and 18 % depending on whether it is assumed that low cost independently produced or expensive patented membrane materials are utilized [18]. One approach has been to reduce the amount of Nafion used by applying a reinforcement to prepare thin but mechanically strong membranes. As a consequence, Gore-Select™ membranes based on polytetrafluoroethylene support impregnated with Nafion have been launched [19,20]. Also several novel partially fluorinated and non-fluorinated alternatives have emerged [21-25]. Radiation-grafted membranes, with varying amounts of fluoride containing aliphatic backbone and typically poly(styrene sulfonic acid) side chains, can belong to either of these groups depending on the composition of the polymer backbone [26-30]. Non-fluorinated candidates are for example sulfonated poly(etheretherketone) or poly(etherketone) consisting of disubstituted phenyl groups separated by –O– and –CO– linkages [31,32] and phosphoric or sulphuric acid doped polybenzimidazole [34-38].

It has been suggested that in the future in PEFCs for stationary applications, where lifetimes of 40 000 h are required, durable Nafion type membranes will be utilized [39]. In contrast, in passenger cars the fuel cell should last for about 5 000 h, which could be satisfied with a less durable but better performing membrane [7,39-41]. Also small-scale applications, such as laptop computers, could offer an opportunity for novel membrane materials: due to the requirements of small size, methanol or some other liquid fuel could be feasible for these devices instead of hydrogen. The methanol permeability through Nafion is, however, rather high [42-46] and, therefore, membranes less permeable to methanol have been sought. Of the aforementioned membranes both radiation grafted [47,48] and polybenzimidazole [35] membranes have been shown to operate under direct methanol fuel cell conditions.

2.4 Open questions

Radiation-grafted membranes have been shown to have interesting properties for the fuel cell applications. In particular conductivities and gas permeabilities comparable to those of the commercial, widely used Nafion membranes can be obtained. The major problem currently appears to be the durability in the fuel cell as very varying lifetimes have been reported.

Several research groups have investigated this type of membrane applying their own starting materials and preparation methods, and properties have often been investigated as a function of the degree of grafting or the ion exchange capacity. As the starting polymer matrix for radiation-grafting films of poly(vinylidene fluoride), PVDF [49,50], poly(tetrafluoroethylene-*co*-hexafluopropylene), FEP [28,29], poly(ethylene-*alt*-tetrafluoroethylene), ETFE [51], and poly(tetrafluoroethylene-*co*-perfluorovinylether), PFA [52], have been used. However, the preparation conditions affect the membrane properties [26], and therefore it is difficult to compare the results reported by different groups for the resulting membranes. In fact the role of the matrix material itself has remained unclear.

In the framework of this project, the suitability of the radiation-grafted membranes for the PEFC and the DMFC, including the role of the matrix material, has been clarified [49,53]. In this context a combination of micro-Raman [54] and X-ray spectroscopies [55] were employed to elucidate changes in the structure of the membranes induced by the fuel cell tests. In addition, the suitability of scanning electrochemical microscopy (Publication VI) to investigate proton transport in the ionically conducting membranes was researched.

This thesis concentrates on determining the influence of the matrix material and the thickness of the matrix film on the physicochemical and the electrochemical properties of radiation-grafted membranes including their applicability both for the hydrogen fuelled PEFC and the DMFC (Publications I and III-VI and the previously unpublished results in Chapter 5). The degradation of the membranes under the hydrogen fuelled PEFC conditions and the effect of crosslinkers on the stability of PVDF based membrane, the most investigated matrix material in the context of this project, are also considered (Publication II).

3. Materials under research

3.1 Preparation of the membranes: irradiation, grafting, and sulfonation

The research and development of alternative polymer electrolyte membranes for fuel cells in this project have been commenced by choosing a radiation-grafting method for membrane preparation and a partially fluorinated poly(vinylidene fluoride), PVDF, film as a starting matrix material [49]. Radiation-grafting is a relatively simple method of modifying and functionalizing commercially available polymer films and offers the direct benefit of avoiding the processing of functionalized polymers consisting of two or more inherently incompatible macromolecules. In addition a high degree of control over the process is attained, and therefore the properties of the membranes can readily be modified. As to the PVDF films, they are commercially available within a competitive price range and have good stability thus offering a suitable matrix for the radiation-grafting reaction.

In radiation induced grafting active sites are created in the matrix polymer film by irradiating with electromagnetic radiation, such as gamma or X-rays, or charged particles, for example electrons or protons [56]. The matrix film can either be exposed to irradiation together with the monomer to be grafted, in which case the grafting reaction takes place immediately (simultaneous grafting), or alone (pre-irradiation grafting). In the latter case, after the irradiation, the polymer containing active sites is transferred into a grafting medium, where the chemical reaction between the active sites and a monomer, such as styrene, takes place. In order to make the grafted membrane ionically conducting, the graft side chains formed are functionalized by sulfonation, typically in a chlorosulfonic acid solution [26-30]. A tentative chemical structure of this kind of material is shown in Figure 2.

The grafting proceeds by a reaction front mechanism: the first grafts are formed near the surfaces of the membrane, after which the monomers proceed through the grafted zones reacting both with the propagating graft chains and the irradiated matrix polymer towards the centre of the membrane [56]. To ensure transport of the ions through the functionalized membrane, the two reaction fronts have to meet and form a penetrating graft network. The structure of the final membrane is affected by numerous factors during the different stages of the preparation, such as the absorbed radiation dose, the reaction temperatures, the monomer concentration in the grafting medium, and the diluents employed for the grafting and the sulfonation. Hence, the preparation conditions should be investigated and chosen with care.

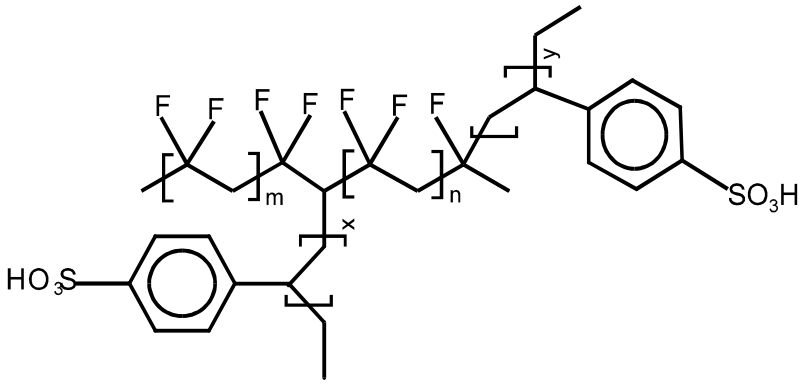

Figure 2. A tentative chemical structure of a radiation-grafted PVDF based proton conductive membrane, PVDF-g-PSSA. The PVDF matrix has been grafted with styrene monomers and subsequently sulfonated.

3.2 Membranes studied

The membranes under study were prepared using the three stage pre-irradiation method, which has been found to be a good method for semi-crystalline materials, where the trapped radicals, created upon irradiation, may have a relatively long lifetime [57]. With this method the formation of homopolymers is lower than in the case of the simultaneous irradiation grafting, and therefore very pure graft copolymers can be prepared.

The details of the preparation of the membranes are given in Publication I and in reference [58]. Briefly, the matrix polymer film was irradiated with an electron beam under inert nitrogen atmosphere, after which it was placed into a styrene solution in order to covalently attach the polystyrene grafts on the active sites. Subsequently the formed side chains were sulfonated with a chlorosulfonic acid solution. The result of grafting is denoted by the degree of grafting (DOG), which is defined as the mass of styrene added to the matrix film:

$$DOG = 100 \cdot \frac{m_{grafted} - m_{initial}}{m_{initial}} \qquad (2)$$

Another variable characterizing the membrane properties is the ion exchange capacity (IEC), which reveals the total amount of sulfonic acid groups in the membrane:

Table 1. Structures, degrees of grafting (DOG), ion exchange capacities (IEC), and thicknesses (l) of the experimental membranes used in this study.

Membrane	formula of the matrix material	DOG/ %	IEC/ meq g^{-1}	l(wet)/ µm	l(dry)/ µm
PVDFa-g-PSSA	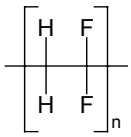	36	1.8	130	90
PVDFb-g-PSSA	id	39	1.8	70	55
PVDFc-g-PSSA	id	36	1.6	35	25
PVDF-co-HFP(6%) -g-PSSA	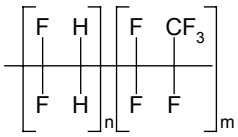	33	1.8	130	90
PVDF-co-HFP(15%) -g-PSSA	id	39	1.9	120	80
FEP-g-PSSA	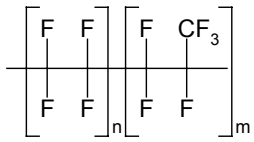	34	1.8	145	80
ETFE-g-PSSA	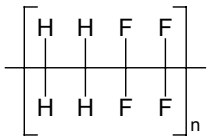	36	1.5	90	55
Nafion 105	-	-	1.0	150	120
Nafion 115	-	-	0.9	150	130
Nafion 117	-	-	0.9	210	180

$$IEC = \frac{n_{SO_3^-}}{m_{grafted+sulfonated}} \quad (3)$$

When investigating the role of the matrix fluoropolymer, PVDF, poly(vinylidene fluoride-*co*-hexafluoropropylene) or PVDF-co-HFP containing 6 and 15 % HFP, FEP, and ETFE were chosen as starting matrix materials. In addition, PVDF films of three different thicknesses were used to elucidate the effect of thickness of the fluoropolymer matrix on the membrane properties. All of the matrix polymers contained fluorine because of the superior thermal and oxidative stability. However, the amount of fluorine or the fluorine to hydrogen ratio as well as the crystallinity and the transition temperatures of the polymers varied. Properties of the resulting membranes and Nafions, used as well-known reference materials, are listed in Table 1.

Most of the results reported in Chapter 4 as well as all data in Publications I and III-V are obtained with the membranes shown in Table 1. These radiation-grafted membranes were prepared under similar conditions, only varying the dose, such that samples with comparable DOGs were obtained (Publication I). The methanol permeability measurements in Chapter 5 and the previously unpublished fuel cell test in Chapter 4.4 as well as results in Publication VI were, however, carried out with 70 μm thick (wet) PVDF, 130 μm PVDF-co-HFP(6%) and 130 μm PVDF-co-HFP(15%) based membranes. These were prepared from 50 μm thick polymer films, and had slightly lower DOGs than those listed in Table 1, about 27 %, and IEC of 1.4 meq g^{-1}. These membranes with lower DOGs were adopted since a decrease of the DOG is shown to increase the durability of these radiation-grafted membranes [59].

Membranes based on PVDF, the most investigated material within this project, were used when studying the effect of crosslinkers on the membrane stability under fuel cell conditions in Publication II. The non-crosslinked membranes had a high DOG of 60 % and thickness of 150 μm (denoted X1-I and X1-II). Effect of two crosslinkers bis(vinyl phenyl)ethane, BVPE, and divinyl benzene, DVB, were investigated. The crosslinked membranes had similar thicknesses but higher DOGs, 100 % and 89 %, respectively, in order to obtain conductivities close to those of the non-crosslinked samples.

4. Physicochemical characterization of the membranes

4.1 Proton conductivity

Proton conductivity is one of the key properties of a polymer electrolyte membrane affecting directly the performance of a fuel cell through ohmic losses and, therefore, in order to attain a high power density, the area resistance of a membrane should be low. All in all conductivity is a complicated process and since the membranes have to operate under dynamic fuel cell conditions it is important to clarify how different factors affect this property. Thus the effects of temperature and relative humidity on ionic conductivities of the membranes were measured in a two-electrode cell, where the membrane was squeezed between Pt electrodes of 3 mm in diameter. A heating jacket of the cell allowed control of the temperature. The RH was regulated by retaining appropriate salt solution or pure water at the bottom of the cell and when measurements were done at 100 % RH, the cell was also flushed with humid nitrogen. The electrodes were connected to an Autolab PGSTAT 20 instrument (Eco Chemie B.V., the Netherlands) equipped with an FRA2 module and an FRA 2.4 software. The complete impedance spectra were recorded in the frequency range of 1 to 900 kHz while the range of 5 to 85 kHz was typically utilized to evaluate the resistance of a membrane by extrapolating the data in the Nyqvist plot to the real axis. The conductivity was calculated from this resistance, the thickness of the membrane, and the area of the electrodes. The pre-treatment of the membranes is described in Publications III and IV.

In polymer electrolyte membranes based on sulfonic acid groups the conductivity is related to the membrane properties, such as the IEC and the ability to take in water. Water is needed to solvate the protons from the acid groups, where they are bound by electrostatic forces, while the number of the sulfonic acid groups as well as the interactions between themselves and with the water molecules affect the formation of hydrophilic channels, through which the protons are transported [60]. In addition external conditions, for example temperature and water activity, affect the conditions in the membrane, and therefore have an impact on the conductivity [61]. It has been suggested that when the water content is low in the membrane the protons proceed via a vehicle mechanism, *i.e.* are transported through the membrane together with the water molecules. When the amount of water in the membrane increases at some point the hopping or Grotthus mechanism becomes dominant, *i.e.* protons move by transferring from one water molecule group to another [61].

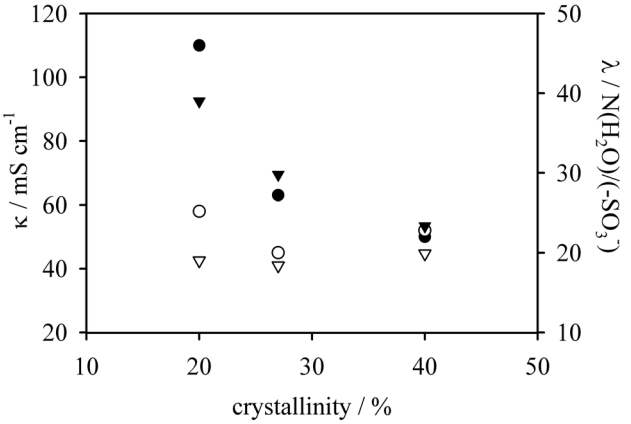

Figure 3. Number of water molecules per sulfonic acid group, λ, and conductivities versus crystallinity in the PVDF and the PVDF-co-HFP based membranes at 100 % RH. Conductivity (●,○) and water uptake (▼,▽) values measured for membranes first boiled in water followed by equilibration with water vapor (filled symbols) and those for the membranes dried before equilibration (open symbols).

The effect of the pre-treatment on the conductivity and the water uptake of the radiation-grafted membranes based on different matrix materials is shown in Figure 3. When the membranes are first boiled in water and thereafter allowed to equilibrate with water vapour, the water uptake appears to be related to the crystallinity of the material. The membranes with larger amounts of flexible amorphous material or lower crystallinity can swell more and thus absorb more solvent. The conductivities follow the same pattern since the amount of bulk-like water increases in the membranes with the amount of absorbed water facilitating the transport of protons [60,61]. The ETFE-g-PSSA membrane was found to deviate from this behaviour (Publication III) due to, at least partly, an evidently lower PSSA concentration at the surface as observed by Raman spectroscopy (Publication V).

However, if the dry membranes are left to equilibrate with water vapour, the differences in the water sorption and in the conductivity are reduced. Apparently the ability of the membranes to take in solvent depends on the conditions. These observations suggest that rearrangements regulated by the crystallinity of a membrane occur when the membrane is immersed in hot liquid water. When a membrane is dried and allowed to equilibrate with water vapour at ambient temperature these rearrangements do not take place, which is reflected in similar water uptakes as well as similar conductivities irrespective of the degree of crystallinity.

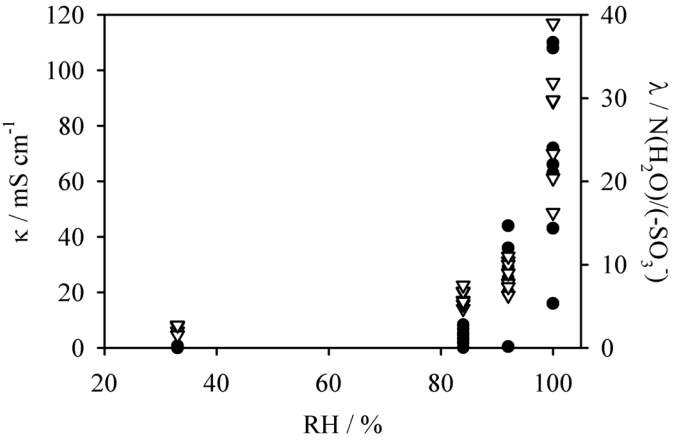

Figure 4. Effect of RH on water sorption (▽) and conductivity (●) of the irradiation- grafted membranes.

The relation between the water uptake and the conductivity in radiation-grafted membranes based on different matrix materials has been considered also in Publication III. Nafion has been included in the study as a well-known reference material. The water sorption curves for the membranes equilibrated with water vapour after boiling appear to be similar and consist of two regions: first the water uptake increases slowly up to around 90 % RH followed by a zone with steeper increase as is indicated in Figure 1 in Publication III. This typical pattern for ion exchange membranes [62,65-68] can be in a simplified way explained as differences in the state of the absorbed water. At the region of slow increment the water first solvates the counter ions from the fixed ionic groups and resides in the primary hydration shell. When more water is absorbed, bulk-like free water starts to accumulate in the membrane swelling the pores and leading to the formation of hydrophilic zones [62,69,70].

The dependence of the water uptake of the membranes, in terms of water molecules per sulfonic acid group, on the relative humidity is shown in Figure 4 together with the conductivities. The conductivities obey a similar pattern to the water sorption *i.e.* at the lower RHs the increase is steady and no significant differences can be observed. However, at around 90 % RH a drastic upturn appears simultaneously with variations in the water uptakes and the conductivities between the membranes. When the RH increases more bulk-like water is introduced in the membrane facilitating transport of the protons [60,61]. The steep increase of the conductivity can be explained by the formation of hydrophilic regions, where the protons are transported, since at the aforementioned RH the membranes have approximately gained the amount of water corresponding non-freezing water bound to the ionic groups (Publication III).

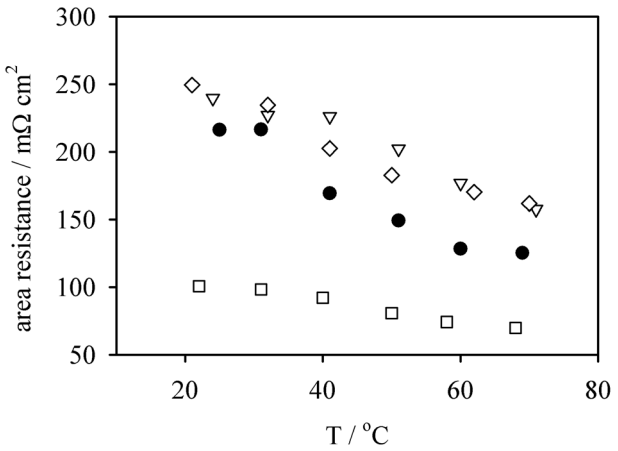

Figure 5. Effect of temperature on the area resistance of the membranes at 100 % RH. Nafion 105 (●), the PVDFa (▽), the PVDF-co-HFP(6%) (◇), and the PVDF-co-HFP(15%) (□) based membranes.

The conductivities of the membranes increased with temperature in the range 20…80°C obeying approximately an Arrhenius law as is described in Publication IV. Again, a similar behaviour has been reported earlier for radiation-grafted membranes [71] as well as for other types of membranes [72-74] resulting from an increase of both the water and the proton diffusion coefficients with temperature in this range [61]. For Nafion the water uptake as function of temperature depends on the pre-treatment and on the humidification conditions [31], and almost constant as well as increasing [65] water uptake with temperature has been reported. The drastic increase in thickness with temperature of the thin PVDFc-g-PSSA (Publication IV) could be a result of increase in water sorption. No further attempt to study this matter was made and the lack of direct evidence restricts more specific conclusions.

From the point of view of an operating fuel cell the changes in the area resistance as a function of temperature are interesting. In Figure 5 it is shown that the area resistances decrease with increasing temperature. This decrease is similar for the three PVDF based membranes with different thickness and for the PVDF-co-HFP(6%)-g-PSSA. The drastic increase of the conductivity of the thin PVDFc-g-PSSA appears to overweight its remarkable thickening with the temperature resulting in a behaviour of the area resistance as function of temperature that is similar to that of the other pure PVDF based membranes. The FEP and the PVDF-co-HFP(15%) based membranes behave in a similar fashion and have a more sluggish decrease of the area resistance than the other membranes due to lesser changes in the thickness. The thickness of the ETFE-g-PSSA membrane increases slightly more than that of the other membranes, excluding the PVDFc-g-PSSA, and a

steeper decrease in the area resistance can be observed. At the highest investigated temperatures the PVDF and the PVDF-co-HFP(6%) based membranes show somewhat higher area resistances than have been suggested for membranes intended for fuel cells [16], but the other ones have resistances low enough for this application.

An idea of the proton conduction mechanism can be obtained by examining water self-diffusion coefficients, D_{H_2O}, and proton diffusion coefficient, D_{H^+}, in the membrane, and therefore the effect of water content of the membranes on these parameters and their interplay were investigated in Publication III. The D_{H_2O} values are roughly similar for all of the membranes with similar water uptakes as can be seen in Figure 6, where the water self-diffusion coefficients measured with pulsed field gradient NMR are depicted as function of the water content in the membranes. It has been shown that the D_{H_2O} is related to the DOG of the radiation-grafted membrane [75] and thus also to the water uptake and/or the IEC. From this point of view Nafion behaves differently because the experimental membranes here have 1.5-2 times higher IECs and therefore a radiation-grafted membrane with a similar IEC and water uptake to Nafion would have a lower D_{H_2O}.

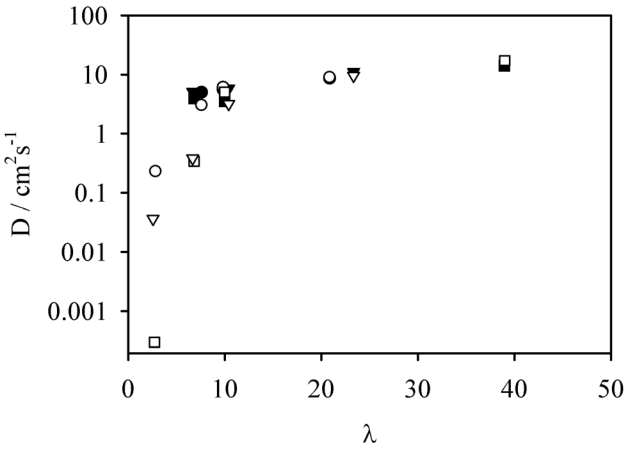

Figure 6. Water self-diffusion coefficients in Nafion 117 (●), PVDFa-g-PSSA (▼), and PVDF-co-HFP(15%)-g-PSSA (■) and proton diffusion coefficients in Nafion 117 (○), PVDFa-g-PSSA (▽), and PVDF-co-HFP(15%)-g-PSSA (□) as a function of λ

In Figure 6 are also shown the D_{H^+} values obtained from the conductivities by applying the Nernst-Einstein equation. They appear to be of the same magnitude and in addition roughly similar to the D_{H_2O} values at the higher water contents. When the amount of water is reduced to around 10 molecules of water per sulfonic acid group, corresponding approximately to the amount of non-freezing water in the membranes, distinct differences appear. While D_{H^+} and D_{H_2O} are still quite similar for Nafion, a gap between them can be observed for the radiation-grafted membranes. The divergences could be due to differences in the structure of these membranes. There is some indication that the radiation-grafted membranes also have the structure typical for an ion exchange membrane [76] with the hydrophilic ionic groups and the water molecules forming clusters surrounded by the hydrophobic matrix polymer [77,78]. The sizes and the forms of the clusters and the hydrophilic proton conducting channels are defined by the ability of the membrane to take in water, the distribution of the side chains and their ability to form clusters. As the water content drops the relatively stiff PSSA side chains may not be able to rearrange but become isolated from the hydrophilic conductivity paths impeding proton transport. Overall, the side-chains in the radiation-grafted membranes can be assumed more incoherently clustered than in Nafion and the hydrophilic regions could be more spread out in between the hydrophobic zones and these fragmented hydrophilic regions are less favourable for proton transport. This image of the structures is supported by data obtained from T_{1H} relaxation times measured with NMR, which can be interpreted to imply that there are essentially solid-liquid interactions in the radiation-grafted membranes while in Nafion also the liquid-liquid interactions are of importance.

A D_{H^+}/D_{H_2O} ratio over 1 is considered as an indication of protons proceeding via a hopping mechanism whereas at lower ratios the vehicle mechanism dominates [61]. For the radiation-grafted membranes the transformation in the conduction mechanism appears to occur only at the maximum water uptake whereas for Nafion some indications of this change are observed at lower water content. However, no major differences between D_{H^+} and D_{H_2O} at the higher water content can be observed and the D_{H^+} values shown here should be interpreted with caution since the acid concentrations in the membranes exceed the generally accepted upper limit for utilizing the Nernst-Einstein equation, which presumes that the ionic groups are fully hydrated.

4.2 Reactant gas permeability

The reactant gas permeability should be low in the membranes to prevent gas mixing and the formation of a mixed potential, which reduces the performance of a fuel cell. Thus the solubility and the diffusion of hydrogen and oxygen in the radiation-grafted membranes based on different matrix materials were studied with a microelectrode cell as described in Publication IV. This kind of measurement setup to investigate oxygen solubility and diffusion in Nafion 117 was first introduced by Parthasarathy *et al.* [79].

The measurements were made under oxygen or hydrogen atmosphere at 100 % RH at a Pt working electrode with a diameter of 50 μm. The gases were humidified at temperature of 50°C and, in addition, extra water was retained in the bottom of the measurement chamber. A dynamic hydrogen electrode [80] consisting of two 300 μm platinum wires, which were sealed in a glass tube, coated galvanostatically with platinum black [81], and connected with a 9 V battery in series with a 3 MΩ resistor, was used as a reference electrode. A platinum mesh electrode served as a counter electrode. All of the electrodes were directly in contact with the membrane as is shown in the scheme of the cell in Figure 7.

Gas permeability data was obtained chronoamperometrically by stepping the potential of the working electrode from the zero current to the mass transfer controlled region of the oxygen reduction or the hydrogen oxidation reaction. Hence, the diffusion coefficients and the solubility could be determined from the current transient by applying the modified Cottrell equation (equation (1) in Publication IV). Tafel slopes and exchange current densities were determined from the mass transfer corrected data obtained from a slow potential sweep from the zero current to the mass transfer limited region of the oxygen reduction reaction.

It is shown [68,82,83] that the diffusion coefficient, D_{O_2}, and the solubility, c_{O_2}, of oxygen are related to the IEC or rather to the water uptake of the radiation-grafted membrane so that the D_{O_2} increases and the c_{O_2} decreases with increasing water uptake. The same trend is also valid for other types of membranes [84] including Nafion [85]. It is generally agreed that this behavior is due to the different solubilities and the diffusion rates of gases in the hydrophilic and in the hydrophobic phases of the membrane [68,82-84,86]. The D_{O_2} is shown to be significantly lower in the hydrophobic PTFE than in water, whereas oxygen dissolves more readily into the former material [85]. PTFE and water can be considered as model materials to estimate the properties of the hydrophobic and the hydrophilic regions in the Nafion membrane, respectively.

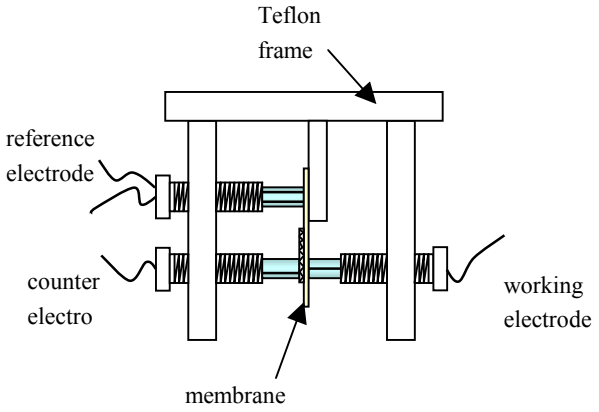

Figure 7. Scheme of the microelectrode cell used to study reactant gas permeability through the membranes.

In these radiation-grafted membranes based on different matrix materials the D_{O_2} values are of the same order of magnitude (Table 3 in Publication IV) even though there are significant differences in the diffusion rates in the pure matrix materials [87]. In addition D_{O_2} appears to be roughly related to the water uptake of these membranes with similar IECs showing higher D_{O_2} at higher water uptakes. This is in agreement with the theory described above suggesting that diffusion occurs in the hydrophobic zones and possibly also in the intermediate phase between the hydrophobic and the hydrophilic zones. However, no clear trend between the water uptake and the c_{O_2} could be detected, which could reflect inherent as well as processing generated differences between the matrix materials themselves since the polymer backbone is regarded to function as a reservoir, in which the oxygen dissolves.

The D_{O_2} value of $1.1 \cdot 10^{-6}$ cm s^{-1} and the c_{O_2} of $9.3 \cdot 10^{-6}$ mol dm^{-3} obtained for Nafion 117 are well in agreement with the results reported under similar experimental conditions, 0.74-2.69·10^{-6} cm s^{-1} and 3.0-26·10^{-6} mol dm^{-3} [79,86], respectively. The thicker Nafion 117 appears to have a slightly lower D_{O_2} but a slightly higher c_{O_2} compared to the radiation-grafted membranes. Instead in Nafion 105, which has a comparable thickness to the thickest of the experimental membranes, D_{O_2} appears to be similar whereas c_{O_2} is still higher than in those membranes.

Water uptakes, quantified as a ratio between mass of the water taken in by the membrane and the mass of the dry membrane, give an idea of the volume ratios of the hydrophobic and the hydrophilic moieties in the membrane. Nafions have lower water

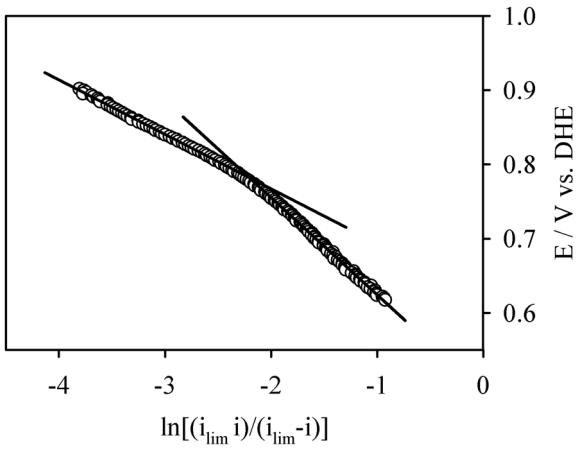

Figure 8. Tafel slopes with distinct regions with slopes of about 60 (high potential) and 120 (low potential) mV dec^{-1} obtained for the PVDFa-g-PSSA under 100 % RH at room temperature.

uptakes than these radiation-grafted membranes (Publication III) and, therefore, they could be assumed to have larger hydrophobic zones in proportion to the hydrophilic ones than the radiation-grafted membranes. This could explain the greater ability of Nafions to dissolve oxygen. The D_{O_2} could also depend on the microstructure of the membranes, which is apparently different for these different types of membranes as discussed in context of the D_{H_2O} and the D_{H^+} in Chapter 4.1.

In the case of hydrogen no clear trend between the membrane properties and the diffusion coefficient, D_{H_2}, or the solubility, c_{H_2}, could be detected (Table 4 in Publication IV). As a smaller molecule hydrogen may be able to permeate through both of the phases in the membrane, and therefore the inherent differences in the membranes can affect these values more than those of oxygen. When comparing the D_{H_2} and the c_{H_2} of the radiation-grafted membranes to those of Nafion 105, it can only be found that they are approximately of the same magnitude.

Because hydrogen is more soluble in these membranes than oxygen, the hydrogen fluxes through the membranes are considerably higher than those of oxygen. No major differences between the oxygen fluxes through the membranes studied could be observed. On the whole the hydrogen fluxes appear to be more unequal than those of oxygen.

In Publication IV it was also observed that the oxygen reduction kinetics at the membrane platinum electrode interface was typical for oxygen reduction on platinum under acidic conditions [88-90]. Accordingly Tafel plots with two different regions with slopes of 60-70 mV dec^{-1} at 0.9-0.8 V vs. DHE and 120-130 mV dec^{-1} at 0.8-0.6 V vs. DHE were recorded corresponding to exchange current densities of the order of 10^{-10}…10^{-9} A cm^{-2} and $l0^{-7}$…10^{-6} A cm^{-2}, respectively, as is shown for the PVDFa-g-PSSA in Figure 8. However, the two membranes with the highest water uptakes, the FEP and the PVDF-co-HFP(15%) based ones, showed slightly higher slopes and lower current densities at high potentials than the other membranes, which was attributed to drying of these membranes [91]. Similar values are reported also for Nafion 117 under the same conditions [79,92]. The alternation in the Tafel slopes imply different absorption isotherms over the investigated potential range [88-90].

4.3 Structure

Surface structure has been suggested to affect the membrane performance [93] as well as the stability of the membranes in the fuel cell [29,94]. Changes in the surface structures induced by grafting and sulfonation of the membranes based on the different matrix materials were detected with atomic force microscopy (AFM), experimental details are given in Publication I. Briefly, the AFM images were obtained with a Topometrix 2000 Explorer Scanning Probe Microscope using a 1660-00 silicon probe. The samples were dried in a desiccator over P_2O_2 since water molecules disturb the measurement when scanning in a non-contact mode, which is suitable for soft samples.

The surfaces of each of the membranes became rougher upon grafting and sulfonation, after which spherical structures could be observed. However, the size of the structures varied greatly from 0.1 to 1 μm even in the PVDF based samples suggesting that the processing of the films may play a role. Any connection between the PSSA side chain distribution (Publication V) or the grafting kinetics and the surface structure of the membrane could not be observed. Since the AFM images emerge from chemical as well as structural interactions between the probe tip and the membrane, caution is needed when interpreting the images.

An electrochemical view of proton diffusion and concentration in the membrane was obtained utilizing scanning electrochemical microscopy (SECM), a method that has not been used earlier to investigate proton conducting membranes. These preliminary studies

were made in the absence of electric field and with a rather large working electrode tip (diameter of 25 μm), but in the future electrical field could be added in order to obtain conditions resembling those in an operating fuel cell. To obtain better resolution a smaller tip could be utilized.

The details of the experiment are given in Publication VI. In short, prior to the measurement the membranes were equilibrated in a deoxygenated KCl-HCl solution. Surface images and approach curves were measured with the SECM by applying a potential on the tip such that the proton reduction reaction was mass transfer limited. In addition current transients were measured by stepping the tip from equilibrium to a mass transfer limited potential. Both the concentration and the diffusion coefficient of hydrogen ions in the membranes were estimated by interpreting the obtained data with an earlier developed model for a system consisting of two homogeneous immiscible phases [95].

The surfaces of the membranes appeared to be inhomogeneous as expected on the basis of the earlier AFM (Publication I) and the micro Raman (Publications II and V) measurements. On the bases of the approach curves and the current transients a rough image of proton transport across the surface was obtained, indicating that the membranes based on different matrix materials with similar DOGs of about 27 % had broadly similar proton concentrations and diffusion coefficients when equilibrated with the KCl-HCl solution. The conductivities calculated on the basis of these results were in agreement with those measured with impedance spectroscopy.

The PVDF-g-PSSA membrane with DOG of 60 % showed wider proton concentration range having higher concentrations in regions where higher tip currents were detected. In general the proton concentration in this membrane was twice as high as those in other membranes studied (Table I in Publication VI) while the diffusion coefficients were of the same order. However, the measured conductivity for this membrane appeared to be clearly higher than was expected from the proton diffusion coefficients and the concentrations obtained with the SECM. This was attributed to uptake of KCl and HCl together with water due to higher water uptake in this membrane compared to the other membranes under study.

4.4 Fuel cell tests

In the fuel cell materials are exposed both to reductive and oxidative conditions at elevated temperature in the presence of water. It has been suggested that at the cathode oxygen adsorbed on the platinum electrode react by forming adsorbed $HO_2\cdot$ radicals [15,88-90,96-

100] and apparently small amounts of H_2O_2 [96,97,99,100] whereas at the anode hydrogen is dissociatively chemisorbed and the hydrogen atoms are subsequently electrooxidised [15,101]. A membrane degradation mechanism resulting in faster degradation on the anode side has been proposed [93,102,103] even though the products from the cathode reaction are considered especially detrimental for some membranes [93,103,104]. The contradiction has been explained by oxygen diffusion through the membrane to the anode where reactions leading to the degradation of a membrane occur. Preliminary information about the chemical durability of a membrane in an oxidative environment can be obtained by exposing the membrane to a hydrogen peroxide solution while mechanical tests can provide an idea about the mechanical strength of a membrane. However, the actual durability of the membranes in a fuel cell is difficult or even impossible to predict without testing under real fuel cell conditions.

To investigate behaviour of the radiation-grafted membranes under fuel cell conditions tests were carried out in a single celled fuel cell with 5 cm^2 active area (GlobeTech, Inc, USA, later on incorporated into ElectroChem, Inc., USA) connected with an Amrel EL 1132 electronic load (American Reliance, Inc., USA), which was controlled via a homemade LabView® (National Instruments, USA) based measurement program [50]. The temperature of the cell was regulated with an 1/16-DIN temperature controller (West Instruments, UK) via a K-type thermocouple while humidification of pure hydrogen and oxygen were carried out in a modified humidification sub-system purchased from GlobeTech. The membranes were clamped in the cell together with the gas diffusion electrodes (single sided ELAT® electrodes containing 0.4 mg Pt cm^{-2} from E-TEK, USA), which were covered with a Nafon solution (0.6-0.8 mg cm^{-2}), with a standard torque of 5.5 Nm. Hot-pressing was omitted since the samples were required for further studies with Raman and X-ray spectroscopies after the fuel cell tests and, therefore, the electrodes had to be readily removable after the tests. The steady state polarization curves were measured galvanostatically by changing the current density in steps of 5 mA cm^{-2} after the potential was stabilized from zero up to a value where the cell voltage dropped below 0.3 V. Durability of the membrane was investigated by keeping the cell at 0.4 V and following the changes in the current until the current density fell clearly below 100 mA cm^{-2}.

Depicting the distribution of the PSSA groups in the fuel cell tested radiation-grafted membranes could give an indication about the progress of the degradation of the membranes. Since crosslinking was shown to improve durability of the radiation-grafted membranes [93,105,106] the effect of two crosslinkers, bis(vinyl phenyl)ethane, BVPE, and divinyl benzene, DVB, on the durability of PVDF based membranes was investigated (Publication II). However, the DVB crosslinks rendered the PVDF based membrane so brittle that it failed within few hours time in the fuel cell in spite of the similar tear

strengths of the wet crosslinked membranes [107]. The BVPE crosslinked membrane proved to be mechanically more suitable, but considerably longer lifetimes were not attained compared to the non-crosslinked PVDF-g-PSSA. Yet the crosslinking appeared to protect the side of the membrane facing the anode, which had a higher PSSA concentration, here and there even similar to that in the pristine sample, than the cathode side after the fuel cell test (Figure 7 in Publication II). Perhaps the less flexible structure protects the anode side by decreasing both the mechanical stress and the chemical degradation due to lower water uptake and the different structure of the ionic aggregates [78]. However, loss of conductivity due to the loss of the percolating PSSA network limited the lifetime of this membrane.

After the fuel cell test the non-crosslinked PVDF-g-PSSA membranes also showed higher PSSA concentrations on the anode side (Figures 3, 5, and 6 in Publication II) together with major loss of PSSA at the boundary between the electrode covered active and the gasket covered inactive zones. This supported the conclusion that the chemical degradation is induced by species developing during the oxygen reduction and diffusing into the membrane and is expedited by mechanical stress due to changes in the water balance in the membrane, which is most intense between the active and inactive regions. In contrast, according to the generally suggested degradation mechanism the anode side should degrade faster but the direct evidence supporting this was obtained in an electrolysis cell [16, 94, 108], and therefore the results could be only extrapolated to the fuel cell behaviour.

The role of the matrix material in the behaviour of the radiation-grafted membranes under fuel cell conditions was investigated in Publications IV and V. The durability tests of all of the experimental membranes were terminated by a sharp drop in current density except that of the ETFE-g-PSSA, whose performance decreased gradually over a period of 100 h. The matrix material appeared to have an influence on the durability of the radiation-grafted membrane: the most amorphous ones showed the shortest lifetimes. In addition, the matrix polymer of the thinnest of the PVDF based membranes could not offer as much mechanical support as the thicker membranes and, therefore, it had a shorter lifetime.

As a result of the fuel cell test, all the membranes degraded chemically by losing the entire PSSA moieties, which was reflected in proton conductivities of less than 1 mS cm^{-1} in the tested membranes (Publication V). PSSA was lost almost completely in all of the membranes despite different lifetimes in the cell, indicating that degradation proceeded at different rates. In addition to chemical degradation, all of the membranes failed mechanically at the interface of the active and the inactive areas. However, ETFE-g-PSSA showed a different behaviour in both respects: an insulating layer was developed on its

surface during the fuel cell test and no mechanical failure could be observed. Apparently the layer formed protected the membrane from the chemical degradation.

The fast failure appeared to be accompanied by distinct structural deformation in the matrix polymer: the chain structure of the PVDFc and the PVDF-co-HFP(15%) based membranes were altered while the FEP-g-PSSA apparently had lost some amorphous material. The amount of amorphous material in the ETFE-g-PSSA had also decreased, which could party be attributed to the small amount of PSSA remaining in the membrane. However, both FEP and ETFE have a phase transition around the temperature used for fuel cell test [109], which could induce this different behaviour.

According to the hydrogen peroxide tests the chemical degradation is facilitated by a large water uptake of the membrane, which increases the reaction surface [53], explaining partly the faster degradation of those membranes with higher water uptakes and, perhaps, that of the thin PVDFc-g-PSSA, the water uptake of which might have increased with temperature. However, these relatively amorphous membranes also experience more violent mechanical forces induced by the chemical degradation and the local variations of the fuel cell conditions as indicated by the structural changes in the matrix polymer. In addition the chemical degradation is pronounced at the interface between the active and the inactive regions where cracks were formed. In conclusion, this supports the earlier conclusions that the degradation is probably an interplay between these two phenomena, mechanical and chemical degradation.

When comparing the duplicates of the PVDF-g-PSSA samples tested 200 h in a fuel cell at 0.4 V the one showing a higher current density during the cell operation had lost less PSSA groups during the test period (Figures 3 and 4 in Publication II). Since the membranes and the other fuel cell components were identical the differences in the current density must be induced by dissimilar contacts in the cell, especially between the gas diffusion electrodes and the membranes. This suggests that a better contact with gas diffusion electrodes protects the membrane either by diminishing mechanical stress or chemically due to a protecting effect of the Nafion coating at the gas diffusion electrode surface [103]. An idea of how much this could affect the lifetime, was obtained when duplicating fuel cell tests of the membranes based on different matrix materials (Publications IV and V). Lifetimes were in general within 10 hours but one of the PVDF-co-HFP(6%) based membranes showed several times longer lifetime than its counterparts. This was attributed partly to differences in the sealing and partly to the electrode membrane contacts.

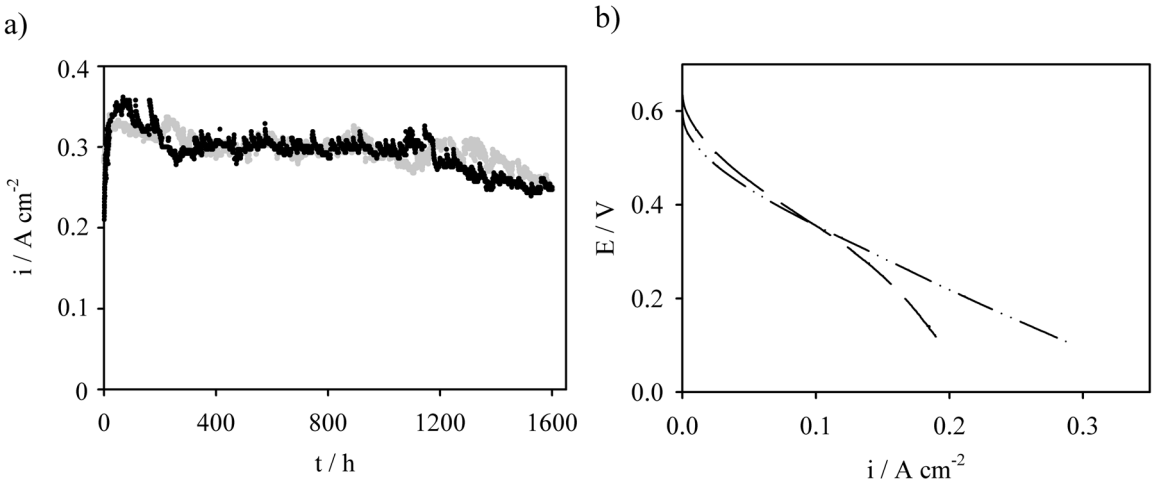

Figure 9. a) 1600 h constant voltage tests (0.4 V) and b) polarization curves for the PVDF (black) and the PVDF-co-HFP(6%) (grey) based membranes with DOG ≈ 30%. The non-pressurized fuel cell operated at 70°C with 1 ml min H_2/O_2 feed.

Since indications of longer lifetimes of the radiation-grafted membranes can be found [103,110] the cell construction was improved after the aforementioned test series by changing the gasket material, lowering the clamping pressure to 4 Nm, modifying the humidifying unit, and using membranes with lower DOGs. New polarization curves with similar trends to those seen earlier were obtained but the lifetimes of the membranes were improved. The performances of the PVDF and the PVDF-co-HFP(6%) based membrane shown in Figure 9 were quite similar but so were also their area resistances at the temperature of 70°C. The lifetimes are not yet long enough for practical applications, but can apparently be much improved by optimising the cell construction and the structure of the membranes. However, this was outside the scope of this thesis.

5. Applicability of irradiation grafted membranes to direct methanol fuel cell

5.1 Operation principle of a direct methanol fuel cell

As a gaseous fuel, hydrogen is relatively difficult to handle, deliver, and store and, therefore alternative liquid candidates, for example methanol, are being investigated especially for portable applications, such as laptop computers and video cameras, and for passenger cars where the size is an issue [111-113]. Methanol is a low cost and electrochemically fairly reactive compound with energy density of the same order as in fuels commonly used in vehicles [42]. Thanks to these properties it is considered as a competitive alternative fuel for the PEFC.

A direct methanol fuel cell (DMFC) is constructed like a conventional PEFC, the main difference being the fuel utilized. In the case of a DMFC the anode is fed with a dilute aqueous methanol solution, typically 1 mol dm^{-3}, or vaporized methanol. In order to have as small storages and total systems as possible higher methanol concentrations with smaller water reservoirs would be feasible. However, methanol permeability through the membrane restricts the optimal operation concentrations to low value. The permeability increases with increasing methanol concentration reducing the cathode potentials as a consequence of competing electrochemical processes. The cathode structure may also become flooded [113], and then the oxygen diffusion to electrocatalyst is more difficult reducing the obtainable current densities even further. In addition, part of the fuel is wasted unless an efficient, and complicated, circulation system is constructed.

At the anode methanol is oxidised on a platinum-ruthenium electrocatalyst releasing carbon dioxide and heat in addition to protons and electrons:

$$CH_3OH + H_2O \rightarrow CO_2 + 6\ H^+ + 6\ e^- \qquad E^\circ = 0.016\ V \qquad \text{(iv)}$$

The reaction at the cathode is the same as in a PEFC, reaction (ii), resulting in the overall reaction:

$$CH_3OH + 3/2\ O_2 \rightarrow CO_2 + 2\ H_2O \qquad \text{(v)}$$

This reaction has a standard potential of 1.21 V. However, OCPs obtained today are substantially lower owing to a combination of the above-described problems with methanol

permeability and sluggish reaction kinetics at both electrodes. The latter problem can be reduced by careful design of the electrodes [113] whereas searching for novel, less methanol permeable membrane alternatives, might solve the first one. Both these problems could be avoided by utilizing a reformer to convert methanol into a hydrogen rich gas prior to feeding the fuel into the fuel cell, which yet complicates the system even more. However, reformers could be used in the medium size application, *e.g.* vehicular applications, whereas in the smaller applications direct methanol feed to the fuel cell would be preferred.

5.2 Methods to determine methanol permeability

Since one of the major problems concerning the DMFC is the methanol permeability through the polymer electrolyte membrane, the applicability of the radiation-grafted membranes as well as the effect of the matrix material on the behaviour of the membranes in the DMFC can be evaluated by determining this quantity. Several methods have been used to investigate methanol permeability through proton conducting membranes. The simplest one involves two compartments filled with solutions of unequal methanol concentrations, which are separated by a proton conducting membrane [114,115]. More realistic conditions are obtained utilizing a fuel cell under OCP with one of the compartments fed with methanol solution and the other with gas [116]. The permeability is determined from changes in the methanol concentrations brought about by diffusion, while the evaluation of the diffusion coefficient and the concentration of methanol in the membrane is possible in the liquid-membrane-liquid type of construction by applying electrochemical methods [114].

A very sophisticated method to determine methanol permeability as function of current density under real DMFC conditions is described by H. Dohle *et al*. [117]. In addition to measuring current density as a function of potential, this complicated system involves evaluation of the carbon dioxide fluxes in the cell and as a result the methanol permeation through the membrane is obtained. However, the contributions of the diffusion coefficient and the methanol concentration in the membrane to the permeability, which would be interesting to determine in the case of novel membrane materials, remain unclear.

Ren *et al.* [118] have introduced a method to evaluate the diffusion coefficient and the concentration of methanol in the membrane under open-circuit conditions utilizing fuel cell hardware for the measurements. Data obtained from the electrochemical measurements is corrected for electro-osmotic drag obtained from water-methanol drag coefficients, *i.e.*

the number of water and methanol molecules per proton transported through the membrane. This last method has been chosen to investigate methanol permeability, since it offers the possibility to determine both the diffusion coefficient and the concentration of methanol in the membrane in a real fuel cell environment.

5.3 Water drag coefficient

Effect of the membrane on the water transport is an important factor in a DMFC both in the respect of conductivity and methanol permeability since methanol permeates through the membrane together with water. Water transport through the membrane in polymer electrolyte fuel cells is induced by different phenomena: diffusion is generated by an activity gradient across the membrane, while migrating protons bring forth electro-osmotic drag when the cell is under current. If a pressure difference exists across the membrane, also hydraulic forces play a part.

Here a method developed by Ren *et al*. [119] is utilized to determine the water drag coefficients in a DMFC with a methanol solution feed to the anode and dry oxygen feed to the cathode. During the measurements equal back pressures on the cathode and the anode compartments of the cell are applied in order to prevent water transport being induced by a pressure difference. At sufficiently high current densities, depending on the cell conditions, water accumulating at the cathode due to cathode reactions and electro-osmotic drag attains an activity of unity eliminating diffusive transport. Under these conditions the measurable water flux across the membrane is exclusively driven by electro-osmotic drag. The amount of water transported through the membrane is obtained from the total water flux from the cathode taking into account water formed upon oxygen reduction and the oxidation reaction of the permeated methanol, while the number of protons is calculated from the measured cell current.

Water drag coefficient measurements were carried out galvanostatically in a single celled fuel cell with an active area of 5 cm^2 (Fuel Cell Technologies, Inc., USA) connected with an Autolab PGSTAT 20 instrument (Eco Chemie B.V., the Netherlands) equipped with GPES 4.8 software. Gas diffusion electrodes (single sided ELAT® electrodes by E-TEK, USA) had 2.0 mg Pt-Ru alloy cm^{-2} at the anode and 1.0 mg Pt cm^{-2} at the cathode, and were coated with a Nafion solution (5 weight per cent, Aldrich, USA) so that the Nafion content was 0.6-0.8 mg cm^{-2}. The electrodes were hot-pressed onto the membrane (120^{o}C, 10 kN, 2 min) to prevent Nafion dissolution and to improve the contact. The cell was operated at constant current with 1 or 3 mol dm^{-3} methanol (LiChrosolv®, Merck,

USA) aqueous solution feed to the anode at 2 ml min^{-1} and dry oxygen (AGA) to the cathode at 270 ml min^{-1}. The methanol flow was controlled with a Reglo-CPF Digital pump (Ismatec, Switzerland) while the oxygen supply was regulated via a 5850S mass flow controller (Brooks Instruments, USA). Experiments were carried out at 30, 50, and 70°C with equal back pressures of 1 bar(g) at the anode and the cathode compartments. The water emerging from the cathode was trapped with a $CaSO_4$ based Drierite® drying agent giving the total amount of water exiting. The CO_2 flux from the cathode outlet was detected with a nondispersive linearized GMM-12B CO_2 sensor (Vaisala, Inc, Finland) while the flow rate was measured with a 5860S mass flow meter (Brooks Instruments, USA) to determine the amount of water generated upon methanol oxidation. The cell was allowed to stabilize for 0.5 h at a constant current prior to a 1.5 h water trapping period.

5.4 Methanol permeability

The principle of the determination of methanol permeability is to measure the amount of methanol transported through the membrane in the fuel cell by oxidizing the permeated methanol under an inert environment at the other compartment of the cell as described by Ren *et al*. [118]. These measurements were carried out with the same equipment used in the water drag coefficient determination. The methanol flow conditions were equal to those employed in the drag coefficient measurements but the oxygen feed was replaced with humidified nitrogen at 270 ml min^{-1}. However, the methanol compartment was not pressurized while back pressures of 1.0, 1.5 and 2.0 bar(g) were utilized at the temperatures of 30, 50, and 70°C, respectively, on the nitrogen side. Nitrogen humidification temperatures were 20°C above the cell temperature in order to have liquid water also in the nitrogen compartment of the cell, thus maintaining equal water activity in both compartments of the cell.

The diffusion coefficient, D_m, and the concentration, c_m, of methanol in the membrane were calculated from the limiting currents, I_{lim}, observed for methanol oxidation and from the slope of the current transients $\left|I_t\sqrt{t}\right|_{Cot}$, when the potential was stepped from the equilibrium to the mass-transfer limited region, according to equations (4) and (5) with correction for electro-osmotic drag, k_{dt} and k_{dl}, obtained from the water-methanol drag measurements.

$$D_m = \left(\frac{k_{dt}}{k_{dl}}\right)^2 \cdot \frac{l^2 I_{\lim}^2}{\pi \left[I_t \sqrt{t}\right]_{Cot}^2} \quad (4)$$

$$c_m = \frac{k_{dl}}{k_{dt}^2} \cdot \frac{\pi \left[I_t \sqrt{t}\right]_{Cot}^2}{6FlI_{\lim}} \quad (5)$$

where l is the thickness of the membrane and F the Faraday constant.

5.5 Results

Water drag coefficients determined for the reference material Nafion 115 and for the two radiation-grafted membranes based on different matrix materials with DOG ≈ 27 % are shown in Figure 10. The membrane based on the PVDF-co-HFP(15%) matrix had to be excluded from the study since that matrix could not endure the pressures used in the measurements.

The cell was assembled immediately after hot-pressing the gas diffusion electrodes membrane assembly and, therefore, the data obtained for Nafion 115 can be compared to the results presented for dried, slightly thicker Nafion 117 [120]. The data were found to be well in agreement. Nafion appeared to have lower water drag coefficients than the radiation-grafted membranes. However, the drag coefficient of Nafion was shown to increase with the IEC [120] and these radiation-grafted membranes had 1.5 times higher IECs than Nafion 115 and, therefore, the drag coefficients should not be directly compared. Also the water uptake of Nafion (0.35 g/g) is slightly lower than those of the radiation-grafted membranes, 0.45 and 0.62 g/g for the PVDF-g-PSSA and the PVDF-co-HFP(6%)-g-PSSA, respectively. Therefore the radiation-grafted membranes can be assumed to have larger hydrophilic part with more dispersed water channels compared to Nafion (Publication III), which might facilitate water transport together with the protons. This favouring of the vehicle at the expense of the hopping mechanism results in higher amount of water molecules transported per proton.

As a comparison the changes in the conductivities as a function of temperature for membranes equilibrated with water vapour are also shown in Figure 10. Methanol has been reported to attenuate the conductivity of Nafion [121], and therefore these values can be considered as indicative since the measurements are made for membranes in the absence of methanol. Comparison of the data in Figure 10 for the two radiation-grafted membranes reveals that the water drag coefficients are lower for the PVDF than for the PVDF-co-

HFP(6%) based membrane, but the conductivities are quite similar. The drag coefficient depends on the structure of the membranes reflecting the interactions between the polymer and the water molecules [120,122]. As a more rigid matrix PVDF-g-PSSA can absorb less water than the PVDF-co-HFP(6%) based membrane and, therefore there is less bulk-like water in the first mentioned membrane and the water-membrane interactions are more pronounced resulting in a lower drag coefficient.

The drag coefficients increase with the temperature due to diminishing water-polymer interactions and alter in the proton transport mechanism [31,120,122]. At higher temperatures the hydrogen bonding between the water molecules becomes weaker rendering the proton hopping involved in the Grothus mechanism less favourable and, consequently increasing the contribution of the vehicle mechanism to the proton transport. Since the conductivity increases with the temperature, protons are transported faster, enhancing also the water transport.

Drag coefficients measured using 3 mol dm^{-3} methanol solution feed are quite similar to those measured with the more dilute solution implying, that, at least at these low mole fractions, methanol does not affect the structure of the membranes notably but merely replaces some water molecules. However, the radiation-grafted membranes and Nafion are found to behave differently at higher methanol mole fractions [123].

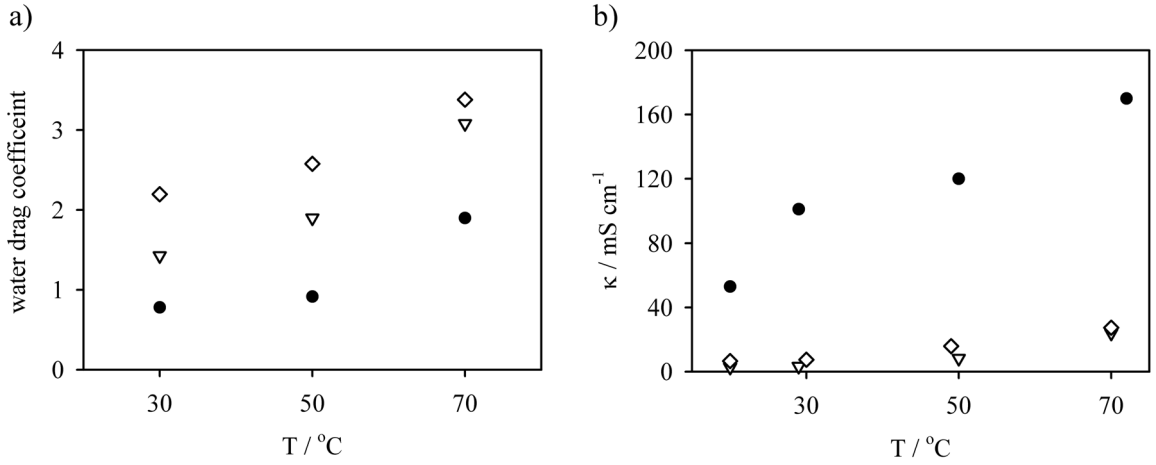

Figure 10. a) Water drag coefficients and b) conductivities as function of temperature for Nafion 115 (●), the PVDF (▽) and the PVDF-co-HFP (◇) based membranes. Water drag coefficient have been measured in a DMFC with 1 mol dm^{-3} methanol solution feed at 2 ml min^{-1} flow rate for the anode and dry oxygen feed at 270 ml min^{-1} for the cathode while the conductivities have been determined under 100 % RH in the absence of methanol.

Table 2. Methanol diffusion coefficients in the membranes at different temperatures with 1 mol dm^{-3} methanol solution feed.

Membrane	$10^6 \cdot D$ / cm^2 s^{-1}		
	30°C	50°C	70°C
Nafion 115	5.9	6.0	6.3
PVDF-g-PSSA	1.5	1.8	2.1
PVDF-co-HFP(6%)-g-PSSA	2.1	3.0	5.6

Methanol diffusion coefficients obtained for Nafion 115 are comparable to those reported for Nafion 117 [47,114,118], and are collected in Table 2 together with values obtained for the radiation-grafted membranes at 1 mol dm^{-3} methanol solution feed. The higher values obtained for Nafion again reflect the differences in the structure between the membrane types. The diffusion coefficients increase slightly with the temperature as expected and are broadly similar at both methanol concentrations for all of the membranes. Diffusion of methanol appears to be slightly faster in the radiation-grafted membrane, PVDF-co-HFP(6%)-g-PSSA, with the more amorphous matrix material. The methanol concentration in the membrane appeared to be 2 to 3 times higher for 3 mol dm^{-3} methanol solution feed than for the more diluted solution. Interestingly, the membranes with higher diffusion coefficients appear to have slightly lower methanol concentrations in the membrane itself.

The resulting methanol permeability and fluxes at 1 mol dm^{-3} methanol solution feed are shown in Figure 11, while the values obtained at 3 mol dm^{-3} solution feed are about three times higher. The methanol permeability has been found to depend on the membrane properties, for example both on the membrane thickness and on the IEC [48,118,124], thus making the comparison between the membranes difficult. Nafion and the PVDF-co-HFP(6%)-g-PSSA membrane have similar thicknesses, 140 and 135 μm respectively, and the differences observed in the permeabilities can be attributed to differences in the microstructures of the membranes. For Nafion it has been found that the methanol permeability increases with the IEC [120]. But even though the radiation-grafted membrane has a higher IEC, 1.4 meq g^{-1} compared to 0.9 meq g^{-1} for Nafion, it shows lower methanol permeability, and flux. Therefore the more dispersed structure of the radiation-grafted film is less favourable to the methanol permeability or the PSSA side chains interact with the methanol molecules [123] reducing the permeability.

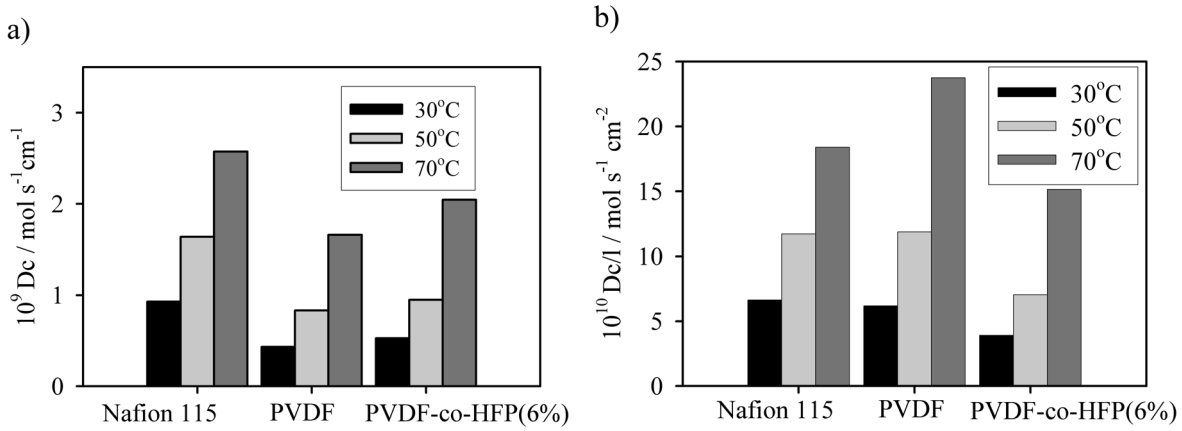

Figure 11. a) Methanol permeability and b) fluxes through the membranes at different temperatures with 1 mol dm^{-3} methanol solution feed with a flow rate of 2 ml min^{-1} and humidified nitrogen feed of 270 ml min^{-1}.

The thicknesses of the initial matrix films of the radiation-grafted membranes were 50 µm, but the thickness of the PVDF-g-PSSA is only half of that of the PVDF-co-HFP(6%) based membrane due to the variations in the water uptake. In contrast to general observations [118,124] the methanol permeability through the thinner membrane is lower than the thicker one. Since the IECs of these membranes are equal the effect is attributed to higher water uptake of the thicker membrane.

When comparing the fluxes shown in Figure 11, it can be seen that the PVDF-co-HFP(6%) based membrane with similar thickness to Nafion has even slightly lower methanol flux than Nafion. Even the thinner, 70 µm thick, PVDF base membrane shows similar fluxes to the thicker Nafion, expect at 70°C. However, in the case of the 3 mol dm^{-3} methanol solution feed, a lower methanol flux for PVDF-g-PSSA than for Nafion is obtained even at 70°C.

The polarization curves for these membranes in the DMFC with 1 mol dm^{-3} methanol solution feed are shown in Figure 12. The high methanol permeability through the Nafion 115 brings the polarization curve of that membrane close to those of the radiation-grafted membranes in spite of the distinctively lower area resistance of Nafion, at least in the water vapour equilibrated membrane in the proton form. In particular, the thinner PVDF-g-PSSA membrane shows equal performances to Nafion. The permeability through the PVDF membrane is slightly lower than through the PVDF-co-HFP(6%) based membrane resulting in a poorer performance of the latter mentioned membrane even though it has slightly lower area resistance. With 3 mol dm^{-3} methanol solution feed polarization curves comparable to Nafion are also obtained. In Figure 12 the effect of the methanol

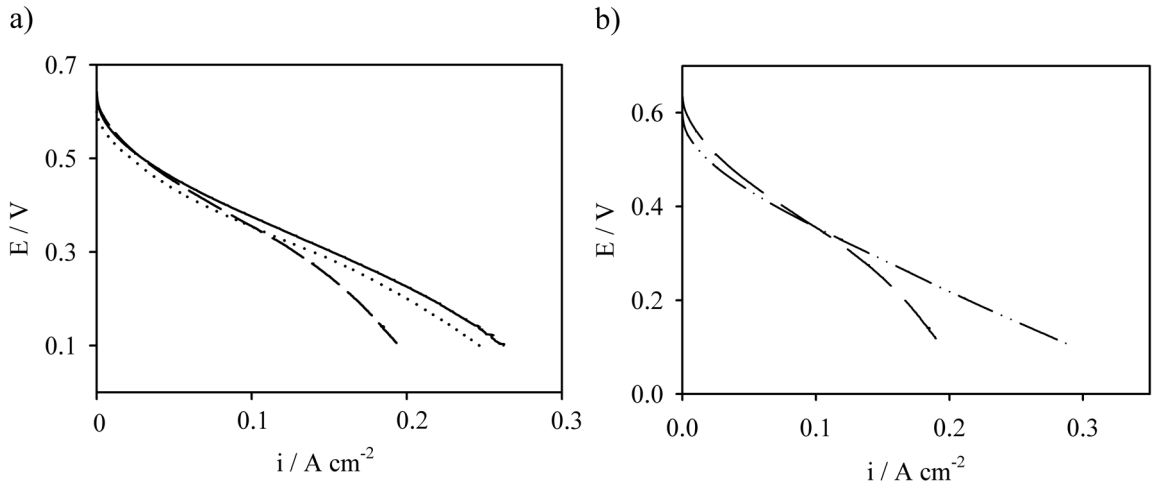

Figure 12. a) Polarization curves for Nafion 115 (solid line), the PVDF (dotted), and the PVDF-co-HFP(6%) (dashed) based membranes at 70°C with 1 mol dm^{-3} methanol solution feed at 2 ml min^{-1} and dry oxygen feed at 270 ml min^{-1}. The anode is not pressurized but the cathode has 1 bar(g). b) Polarization curve for PVDF-co-HFP(6%)-g-PSSA (dotted) is the same as in the adjacent Figure while the other (dash-dotted) curve is measured with 3 mol dm^{-3} methanol solution feed.

concentration on the polarization curve of PVDF-co-HFP(6%)-g-PSSA is also shown. All in all the radiation-grafted membranes perform well in the DMFC, since their methanol permeability is lower than that of Nafion, which compensates for their higher area resistances encountered.

6. Conclusions

The major aim of this work was to determine to what extent the choice of the matrix material affects the properties of the radiation-grafted membrane. It is shown that the properties of the radiation-grafted membranes depend clearly on the preparation conditions [53] and, therefore, results published by different research groups cannot be directly compared.

In the first place it appeared that the major difference brought by the matrix material was the crystallinity of the matrix polymer, which affected the water uptake of the membrane. This in turn influenced such properties of the membrane as conductivity, oxygen permeability, water drag coefficients, methanol permeability, and the actual performance under the fuel cell conditions. The durability of the radiation-grafted membrane also appeared to depend on its chemical and mechanical stability, which are affected by the water content in the membrane. However, the FEP and the ETFE based membranes had a phase transition in the temperature region used for fuel cell tests and their matrix structures collapsed totally. Also the matrix polymers of the most amorphous of the PVDF containing membranes suffered greatly in the fuel cell. The thinnest of the PVDF based membranes was mechanically weak and thus could not sustain the matrix structure unlike the thicker PVDF based membranes. Therefore the durability under the fuel cell conditions could be improved by a proper choice of the matrix material. Apparently too thin polymer films (< 20 μm) should be avoided. In addition, too amorphous matrices or those having a phase transition in the temperature region used were most vulnerable.

Moderate lifetimes can be obtained with this type of membrane under fuel cell conditions with hydrogen as a fuel and pure oxygen as an oxidant. However, research work has to still be done in order to find the best compromise between the structure of the membrane and the performance as well as the durability under the fuel cell conditions. The PSSA side chains should be somehow protected or modified to render them less vulnerable under the aggressive fuel cell conditions. Crosslinking might help to consolidate the membrane structure, but does not necessarily prevent the chemical failure of the membrane. Membrane lifetime can also be prolonged by improving the fuel cell assembly so that the stress experienced by the membrane at the borderline between the active and the inactive areas, where the degradation is more pronounced, decreases. The performance of radiation-grafted membranes under fuel cell condition could be increased by developing electrodes especially for this type of membranes.

When obtaining the above-described results, combining the information obtained from the micro-Raman and the X-ray (wide and small angle X-ray scattering) techniques proved to give versatile insight into changes in the structure of the matrix polymers and in the membranes induced by the preparation [125] and the fuel cell testing. Preliminary studies with the scanning electrochemical microscopy also revealed the applicability of this method to provide direct electrochemical information about the proton transport and the distribution in proton conducting membranes. In future this study could be extended to depict the ion transport phenomena under conditions resembling those in PEFCs and, possibly, the influence of the catalyst layer on the membrane surface could be also investigated.

Some indication of the applicability of the membranes for the direct methanol fuel cell was also obtained. In spite of distinctively higher area resistances, performances close to that of Nafion 115 were obtained with radiation-grafted membranes with relatively low degrees of grafting (≈ 27 %). This was due to structural reasons resulting in lower methanol diffusion and, therefore, also in lower methanol permeability through the radiation-grafted membranes. However, the durability of this type of membrane in the direct methanol fuel cell was not investigated. But as concerns the role of the matrix material, the general observation made in the case of hydrogen fuelled PEFC can be assumed to be valid also in the DMFC.

References

1. U. Bossel, *The Birth of Fuel Cell 1835-1845*, European Fuel Cell Forum, Göttingen 2000, 157 p.
2. *Fuel Cell Handbook*, A.J. Appleby and F.R. Foulkes, Van Nostrand Reinhold, New York 1989, 792 p.
3. A.J. Appleby and E.B. Yeager, *Energy* **11** (1986) 137-152.
4. G. Sattler, *J. Power Sources* **86** (2000) 61-67.
5. C. Hebling and A. Heinzel, *Fuel Cell Bulletin,* July 2002, 8-12.
6. Anon., http://www.fuel-cell-bus-club.com/, 20th March, 2003.
7. M. Doyle and P. Arora, *J. Electrochem. Soc.* **148** (2001) K1-K41.
8. Anon, http://www.daimlerchrysler.com/, 20th March, 2003.
9. Anon, http://www.gm.com/, 20th March, 2003.
10. Anon, *Fuel Cell Bulletin*, January 2003, 2-3.
11. J. Pavio, J. Hallmark, J. Bostaph, A. Fisher, B. Mylan and C.G. Xie, *Fuel Cell Bulletin* **43** (2002) 8-11.
12. J.P. Meyers and H.L. Maynard, *J. Power Sources* **109** (2002) 76-88.
13. Anon, http://www.eia.doe.gov/aer/, 26th March, 2003.
14. M.C. Williams, *Fuel Cell Handbook*, 5th edition, U.S. Department of Energy, Morgatown 2000, 12-4 p.
15. S. Gottesfeld and T.A Zawodzinski, Polymer Electrolyte Fuel Cells in *Advances in Electrochemical Science and Engineering,* R.C. Alkire, H. Gerischer, D.M. Kolb and C.W. Tobias (Ed.), vol 5, Wiley-VCH, Weinheim 1997, pp. 197-301.
16. G.G. Scherer, *Ber. Bunsenges. Phys. Chem.* **94** (1990) 1008-1014.
17. W. Vielstich, *Fuel Cells*, Wiley – Interscience, Bristol 1970, 501 p.
18. I. Bar-On, R. Kirchain and R. Roth, *J. Power Sources* **109** (2002) 71-75.
19. J.A Kolde, B. Bahara, M.S. Wilson, T.A Zawodzinski and S. Gottesfeld, *Proceedings of the 2nd Internationl Symposium on Proton Conducting Membrane Fuel Cells I*, S. Gottesfeld, T. Halpert and A. Landgrebe (Ed.), The Electrochemical Society, New Jersey 1995, pp. 193-201.
20. W. Liu, K. Ruth and G. Rusch, *J. New Mat. Electrochem. Systems* **4** (2001) 227-231.
21. O. Savadogo, *J. New Mat. Electrochem. Systems* **1** (1998) 47-66.
22. M. Rikukawa and K. Sanui, *Prog. Polym. Sci.* **25** (2000) 1463-1502.
23. Ph. Colomban, *Ann. Chim. Sci. Mat.* **24** (1999) 1-18.
24. G. Inzelt, M. Pineri, J.W. Schultze and M.A. Vorotyntsev, *Electrochim. Acta* **45** (2000) 2403-2421.

25. M. Hogarth and X. Glipa, *High Temperature Membranes for Solid Polymer Fuel Cells*, http://www.dti.gov.uk/renewable/pdf/f0200189.pdf, 7th April, 2003.
26. N. Walsby, M. Paronen, J. Juhanoja and F. Sundholm, *J. Appl. Polym. Sci.* **81** (2001) 1572-1580.
27. M.V. Rouilly, E.R. Kötz, O. Haas, G.G. Scherer and A. Chapiro, *J. Membr. Sci.* **81** (1993) 89-95.
28. G.Gebel, E. Ottomani, J.J. Allegraud, N. Betz and A.L. Moël, *Nucl. Instr. and Meth. In Phys. Res. B* **105** (1995) 145-149.
29. M.M. Nasef, H. Saidi and M.A. Yarmo, *J. New Mat. Electrochem. Systems* **3** (2000) 309-317.
30. J.A. Horsfall and K.V. Lovell, *Euro. Pol. J.* **38** (2002) 1671-1682.
31. K.D. Kreuer, *J. Membr. Sci.* **185** (2001) 29-39.
32. J. Kerres, A. Ullrich, F. Meier and T. Häring, *Solid State Ionics* **125** (1999) 243-249.
33. B. Bauer, D.J. Jones, J. Rozière, L. Tchicaya, G. Alberti, M. Casciola, L. Massinelli, A. Peraio, S. Besse and E. Ramunni, *J. New Mat. Electrochem. Systems* **3** (2000) 93-98.
34. C. Pu, W. Huang, K.L. Ley and E.S. Smotkin, *J. Electrochem. Soc.* **142** (1995) L119-L120.
35. J.-T. Wang, J.S. Wainright, R.F. Savinell and M. Litt, *J. Appl. Electrochem.* **26** (1996) 751-756.
36. X. Glipa, M.E. Haddad, D.J. Jones and J. Rozière, *Solid State Ioniocs* **97** (1997) 323-331.
37. X. Glipa, B. Bonnet, B. Mula, D.J. Jones and J. Rozière, *J. Mater. Chem.* **9** (1999) 3045-3049.
38. R. Bouchet and E. Siebert, *Solid State Ioniocs* **118** (1999) 287-299.
39. T.R. Ralph, *Platinum Metals Rev.* **41** (1997) 102-113.
40. B.C.H. Steele and A. Heinzel, *Nature* **414** (2001) 345-352.
41. V. Mehta and J.S. Cooper, *J. Power Sources* **114** (2003) 32-53.
42. C. Lamy, J.-M. Léger and S. Srinivasan, Direct Methanol Fuel Cells: From a Twentieth Century Electrochemist's Dream to a Twenty-first Century Emerging Technology, in *Modern Aspects of Electrochemistry,* J. O'M. Bockris, B.E Conway and R.E. White (ed.), No. 34, Kluwer Academic / Plenum Publishers, New York 2001, pp. 53-118.
43. A. Heinzel and V.M. Barragán, *J. Power Sources* **84** (1999) 70-74.

44. C. Rice, S. Ha, R.I. Masel, P. Waszczuk, A. Wieckowski and T. Barnard, *J. Power Sources* **111** (2002) 83-89.
45. C. Rice, S. Ha, R.I. Masel and A. Wieckowski, *J. Power Sources* **115** (2003) 229-235.
46. K. Yamada, K. Asazawa, K. Yasuda, T. Ioroi, H. Tanaka, Y. Miyazaki and T. Kobayashi, *J. Power Sources* **115** (2003) 236-242.
47. K. Scott, W.M. Taama and P. Argyropoulos, *J. Membr. Sci.* **171** (2000) 119-130.
48. T. Hatanaka, N. Hasegawa, A. Kamiya, M. Kawasumi, Y. Morimoto and K. Kawasumi, *Fuel* (2002) 2173-2176.
49. S. Hietala, *Characterization of Poly(vinylidene-graft-poly(styrene sulfonic acid) Polymer Electrolyte Membrane*, doctoral thesis, University of Helsinki, Department of Chemistry, Helsinki 1999, 41 p.
50. T. Lehtinen, *Physicochemical and Electrochemical Characterization of Partially Fluorinated Proton Conducting Membranes for Fuel Cell*, doctoral thesis, Department of Chemical Technology, Helsinki University of Technology, Espoo 1999, 45 p.
51. H.-P. Brack and G.G. Scherer, *Macromol. Symp.* **126** (1997) 25-49.
52. M.M. Nasef, H. Saidi, H.M Nor and M. Foo, *J. Appl. Polym. Sci.* **76** (2000) 1-11.
53. N. Walsby, *Preparation and Characterization of Radiation-grafted Membranes for Fuel Cells*, doctoral thesis, Department of Chemistry, University of Helsinki 2001, 36 p.
54. H. Ericson, *Novel Material for fuel cells and batteries. Light Scattering studies of the structure and dynamics of Polymer Electrolytes*, doctoral thesis, Department of Experimental Physics, Chalmers University of Technology/Göteborg University 2002, 51 p.
55. K. Jokela, *The Structure of Polymer Based Ion Exchange Membranes and Catalysts by WAXS and SAXS*, doctoral thesis, Department of Physical Science, University of Helsinki 2002, 36 p.
56. A. Chapiro, *Radiation Chemistry of Polymeric Systems*, Interscience Publishers, London 1962, 712 p.
57. X. Zhi-li, W. Gen-hua, W. Han-ing, C. Gyn and N. Min-hua, *Radiat. Phys. Chem.* **22** (1983) 939-945.
58. S. Holmberg, T. Lehtinen, J. Näsman, D. Ostrovskii, M. Paronen, R. Serimaa, F. Sundholm, G. Sundholm, L. Torell and M. Torkkeli, *J. Mater. Chem.* **6** (1996) 1309-1317.
59. P. Gode, J. Ihonen, A. Strandroth, H. Ericson, G. Lindbergh, M. Paronen, F. Sundholm, G. Sundholm and N. Walsby, *Fuel Cells*, accepted.

60. E. Spohr, P. Commer and A.A. Kornyshev, *J. Phys. Chem. B*, **106** (2002) 10560-10569.
61. K.D. Kreuer, *Chem. Mat.* **8** (1996) 610-641.
62. K.K. Pushap, D. Nandan and R.M. Iyer, *J. Chem. Soc.Faraday Trans. 1,* **84** (1988) 2047-2056.
63. T.A. Zawodzinski, Jr., M. Neeman, L.O. Sillerud and S. Gottesfeld, *J. Phys. Chem.* **95** (1991) 6040-6044.
64. T.A. Zawodzinski, Jr., T.E. Springer, J. Davey, R. Jestel, C. Lopez, J. Valerio and S. Gottesfeld, *J. Electrochem. Soc.* **140** (1993), 1981-1985.
65. J.T. Hinatsu, M. Mizuhata and H. Takenaka, *J. Electrochem. Soc.* **141** (1994) 1493-1498.
66. Y. Sone, P. Ekdunge and D. Simonsson, *J. Electrochem. Soc.* **143** (1996) 1254-1259.
67. P.J. James, J.A. Elliott, T.J. McMaster, J.M. Newton, A.M.S. Elliott, S. Hanna and M.J. Miles, *J. Mater. Sci.* **35** (2000) 5111-5119.
68. C. Chuy, V.I. Basura, E. Simon, S. Holdcroft, J. Horsfall and K. Lovell*, J. Electrochem. Soc.* **147** (2000) 4453-4458.
69. K.A. Mauriz, Morphological Theories in *Ionomers; Synthesis, structure, properties and applications*, M.R. Tant, K.A. Mauriz, and G.L. Wilkes (Ed.), Blackie Academic and Professional, London 1997, pp. 95-153.
70. K.A. Mauriz and C.E. Rogers, *Macromolecules* **18** (1985) 483-491.
71. J. Hamlin, F.N. Büchi, O. Haas, M. Stamm and G.G. Scherer, *Electrochim. Acta* **39** (1994) 1303-1307.
72. T.A. Zawodzinski, Jr., C. Derouin, S. Razinski, R.J. Sherman, V.T. Smith, T.E. Springer and and S. Gottesfeld, *J. Electrochem. Soc.* **140** (1993) 1041-1047.
73. Q. Guo, P.N. Pintauro, H. Tang and S. O'Connor, *J. Membr. Sci.* **154** (1999) 175-181.
74. R.W. Kopitzke, C.A. Linkous, H.R. Anderson and G.L. Nelson, *J. Electrochem. Soc.* **147** (2000) 1677-1681.
75. S. Hietala, S.L. Maunu, F. Sundholm, T. Lehtinen and G. Sundholm, *J. Polym. Sci., Part B: Polym. Phys.* **37** (1999) 2893-2900.
76. B.P Grady and S.L. Cooper, Morphological Structure and Characterization in *Ionomers; Synthesis, structure, properties and applications*, M.R. Tant, K.A. Mauriz, and G.L. Wilkes (Ed.), Blackie Academic and Professional, London 1997, pp. 41-94.

77. S. Hietala, S. Holmberg, J. Näsman, D. Ostrovskii, M. Paronen, R. Serimaa, F. Sundholm, L. Torell and M. Torkkeli, *Angew. Makromol. Chem.* **253** (1997) 151-167.
78. M. Elomaa, S. Hietala, M. Paronen, N. Walsby, K. Jokela, R. Serimaa, M. Torkkeli, T. Lehtinen, G. Sundholm and F. Sundholm, *J. Mater. Chem.* **10** (2000) 2678-2684.
79. A. Parthasarathy, C.R. Martin and S. Srinivasan, *J. Electrochem. Soc.* **138** (1991) 916-921.
80. J. Giner, *J. Electrochem. Soc.* **111** (1964) 376-377.
81. D.J.G. Ives and G.J. Janz, *Reference Electrodes: Theory and Practice*, Academic Press, New York 1961, 651 p.
82. T. Lehtinen, G. Sundholm, S. Holmberg, F. Sundholm, P. Björnbom and M. Bursell, *Electrochim. Acta* **43** (1998) 1881-1890.
83. T. Lehtinen, G. Sundholm, and F. Sundholm, *J. Appl. Electrochem.* **29** (1999) 677-685.
84. V.I. Basura, C. Chuy, P.D. Beattie and S. Holdcroft, *J. Electroanal. Chem.* **501** (2001) 77-88.
85. F.N. Büchi, M. Wakizoe, and S. Srinivasan, *J. Electrochem. Soc.* **143** (1996) 927-932.
86. K. Ota, Y. Inoue, M. Motohira and N. Kamiya, *J. New Mat. Electrochem. Syst.* **3** (2000) 193-197.
87. J. Brandrup, E.H. Immergut, and E.A Grulke. *Polymer Handbook*, 4th edition, John Wiley& Sons, New York 1999, p. VI/547.
88. D.B. Sepa, M.V. Vojnovic and A. Damjanovic, *Electrochim. Acta* **26** (1981) 781-793.
89. D.B. Sepa, M.V. Vojnovic, Lj. M. Vracar and A. Damjanovic, *Electrochim. Acta* **31** (1986) 91-96.
90. D.B. Sepa, M.V. Vojnovic, Lj. M. Vracar and A. Damjanovic, *Electrochim. Acta* **32** (1987) 129-134.
91. F.A. Uribe, T.E. Springer and S. Gottesfeld, *J. Electrochem. Soc.* **139** (1992) 765-773.
92. V.I. Basura, P.D. Beattie and S. Holdcroft, *J. Electroanal. Chem.* **458** (1998) 1-5.
93. F.N. Büchi, B. Gupta, O. Haas and G. Scherer, *Electrochim. Acta* **40** (1995) 345-353.

94. G.G. Scherer, E. Killer and D. Grman, *Int. J. Hydrogen. Energy* **17** (1992) 115-123.
95. A.L. Barker, J.V. Macpherson, C.J. Slevin and P.R.Unwin, *J. Phys. Chem. B* **102** (1998) 1586-1598.
96. K.L. Husueh, E.R. Gonzalez and S. Srinivasan, *Electrochim. Acta* **28** (1983) 691-697.
97. C. Fabjan, G. Frithum and H. Hartl, *Ber. Bunsenges. Phys. Chem.* **94** (1990) 937-941.
98. S. Mukerjee, S. Srinivasa and A.J. Appleby, *Electrochim. Acta* **38** (1993) 1661-1669.
99. J.B. Floriano, E.A Ticianelli and E.R. Gonzales, *J. Electroanal. Chem.* **367** (1994) 157-164.
100. O. Antonie and R. Durand, *J. Appl. Electerochem.* **30** (2000) 839-844.
101. J.J.T.T. Vermeijen, L.J.J. Janssen and G.J. Visser, *J. Appl. Electerochem.* **27** (1997) 497-506.
102. D.S. Watkins, Research, Development, and Demonstrations of Solid Polymer Fuel Cell Systems in *Fuel Cell Systems,* L.J.M.J. Blomen and M.N. Mugerwa (Ed.), Plenum Press, New York 1993, pp. 493-530.
103. H. Wang and G.A Capuano, *J. Electrochem. Soc.* **145** (1998) 780-784.
104. G. Hübner and E. Roduner, *J. Mater. Chem.* **9** (1999) 409-418.
105. F.N. Büchi, B. Gupta, O. Haas and G. Scherer, *J. Electrochem. Soc.* **142** (1995) 3044-3048.
106. H.P. Brack, F.N. Büchi, J. Huslage and G.G. Scherer, *Proceedings of the 2nd Internationl Symposium on Proton Conducting Membrane Fuel Cells II*, S. Gottesfeld and T.F. Fuller (Ed.), The Electrochemical Society, New Jersey 1999, pp. 52-65.
107. S. Holmberg, J.H. Näsman and F. Sundholm, *Polym. Adv. Technol.* **9** (1998) 121-127.
108. G.G. Scherer, *Hydrogen Energy Progress VI*, T.N. Veziroglu, N. Getoff, P. Weinzierl (Ed.), International Association of Hydrogen Energy, Vienna 1986, vol 1, pp. 382-389.
109. E. Giannetti, *Polym. Int.* **50** (2001) 10-26.
110. J.A. Horsfall and K.V. Lovell, *Fuel Cells* **1** (2001) 186-191.
111. C. Lamy, E.M. Belgsir and J.-M. Léger, *J. Appl. Electrochem.* **31** (2001) 799-809.
112. B.D. McNicol, D.A.J. Rand and K.R. Williams, *J. Power Sources* **100** (2001) 47-59.

113. M.P. Hogarth and T.R. Ralph, *Platinum Metals Rev.* **46** (2002) 146-164.
114. P.S. Kauranen and E. Skou, *J. Appl. Electrochem.* **26** (1996) 909-917.
115. V. Tricoli, *J. Electrochem. Soc.* **145** (1998) 3798-3801.
116. P. Dimitrova, K.A. Friedrich, B. Vogt and U. Stimming, *J. Electroanal. Chem.* **532** (2002) 75-83.
117. H. Dohle, J. Divisek, J. Mergel, H.F. Oetjen, C. Zingler and D. Stolten, *Abstracts: Fule Cells – Powering the 21st century*, J.B. O'Sullivan (Ed.), Oregon 2000, pp. 126-129.
118. X. Ren, T.E. Springer, T.A. Zawodzinski, and S. Gottesfeld, *J. Electrochem. Soc.* **147** (2000) 466-474.
119. X. Ren, W. Henderson, and S. Gottesfeld, *J. Electrochem. Soc.* **144** (1997) L267-L270.
120. X. Ren and S. Gottesfeld, *J. Electrochem. Soc.* **148** (2001) A87-A93.
121. X.Ren, T.A Zawodzinski Jr., F. Uribe, H. Dai and S. Gottesfeld, *Proceedings of the 2nd Internationl Symposium on Proton Conducting Membrane Fuel Cells I*, S. Gottesfeld, G. Halpert and A. Landgrebe (Ed.), The Electrochemical Society, New Jersey 1995, pp. 284-298.
122. M. Ise, K.D. Kreuer and J. Maier, *Solid State Ionics* **125** (1999) 213-223.
123. S. Hietala, S.L. Maunu and F. Sundholm, *J. Polym. Sci.:Pat B: Polym. Phys.* **38** (2000) 3277-3284.
124. A. Heinzel and V.M. Barragán, *J. Power Sources* **84** (1999) 70-74.
125. K. Jokela, R. Serimaa, M. Torkkeli, F. Sundholm, T. Kallio and G. Sundholm, *J. Polym. Sci. Part B: Polym. Phys.,* **40** (2002) 1539-1555.

Abbreviations

AFM	atomic force microscopy
BVPE	bis(vinyl phenyl)ethane
DHE	dynamic hydrogen electrode
DMFC	direct methanol fuel cell
DOG	degree of grafting
DVB	divinyl benzene
ETFE	poly(ethylene-*alt*-tetrafluoroethylene)
FEP	poly(tetrafluoroethylene-*co*-hexafluopropylene)
HFP	hexafluoropropylene
IEC	ion exchange capacity *i.e.* n (SO_3^{2-})/m(membrane)
RH	relative humidity
OPC	open circuit potential
PEFC	polymer electrolyte fuel cell
PFA	poly(tetrafluoroethylene-*co*-perfluorovinylether)
PSSA	polystyrene sulfonic acid
PVDF	poly(vinylidene fluoride)
SECM	scanning electrochemical microscopy
WU	water uptake

Symbols

c_i	concentration of i
D_i	diffusion coefficient of i
E	potential
F	Faraday constant (96 485 Asmol^{-1})
I	current
i	current density
k_{dl}, k_{dt}	coefficients
l	thickness
m	mass
n	amount of substance
R	resistance
t	time
T	temperature
η	overpotential
κ	conductivity
λ	water uptake / N(H_2O)/(SO_3^{2-})